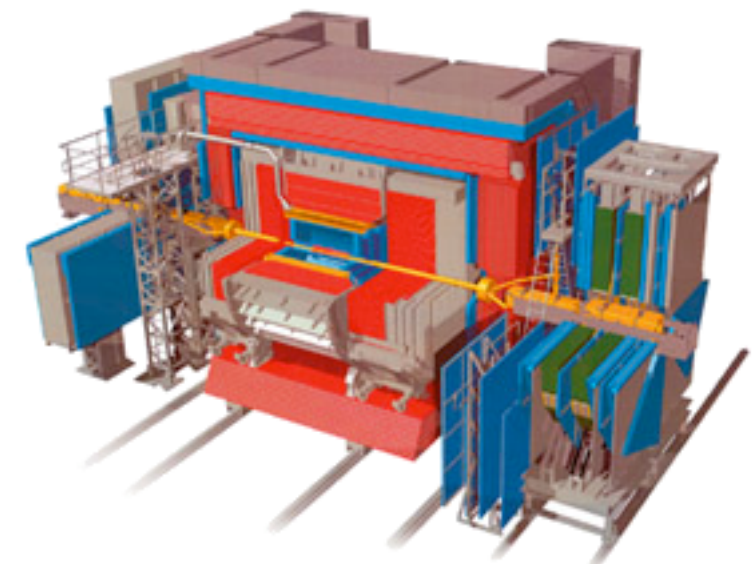
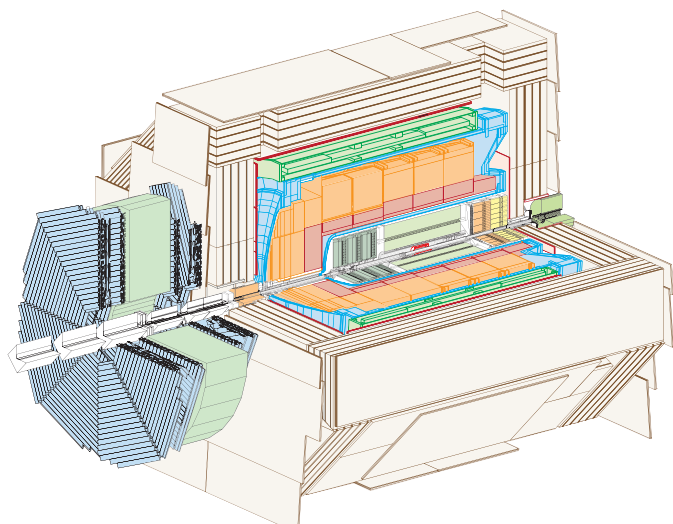


Physics at HERA

DESY Summer Student Lectures
August 15, 2011

Roman Kogler (DESY)
H1 collaboration
roman.kogler@desy.de



Part 2

A Little Bit Of QCD

The QCD Improved Quark Parton Model

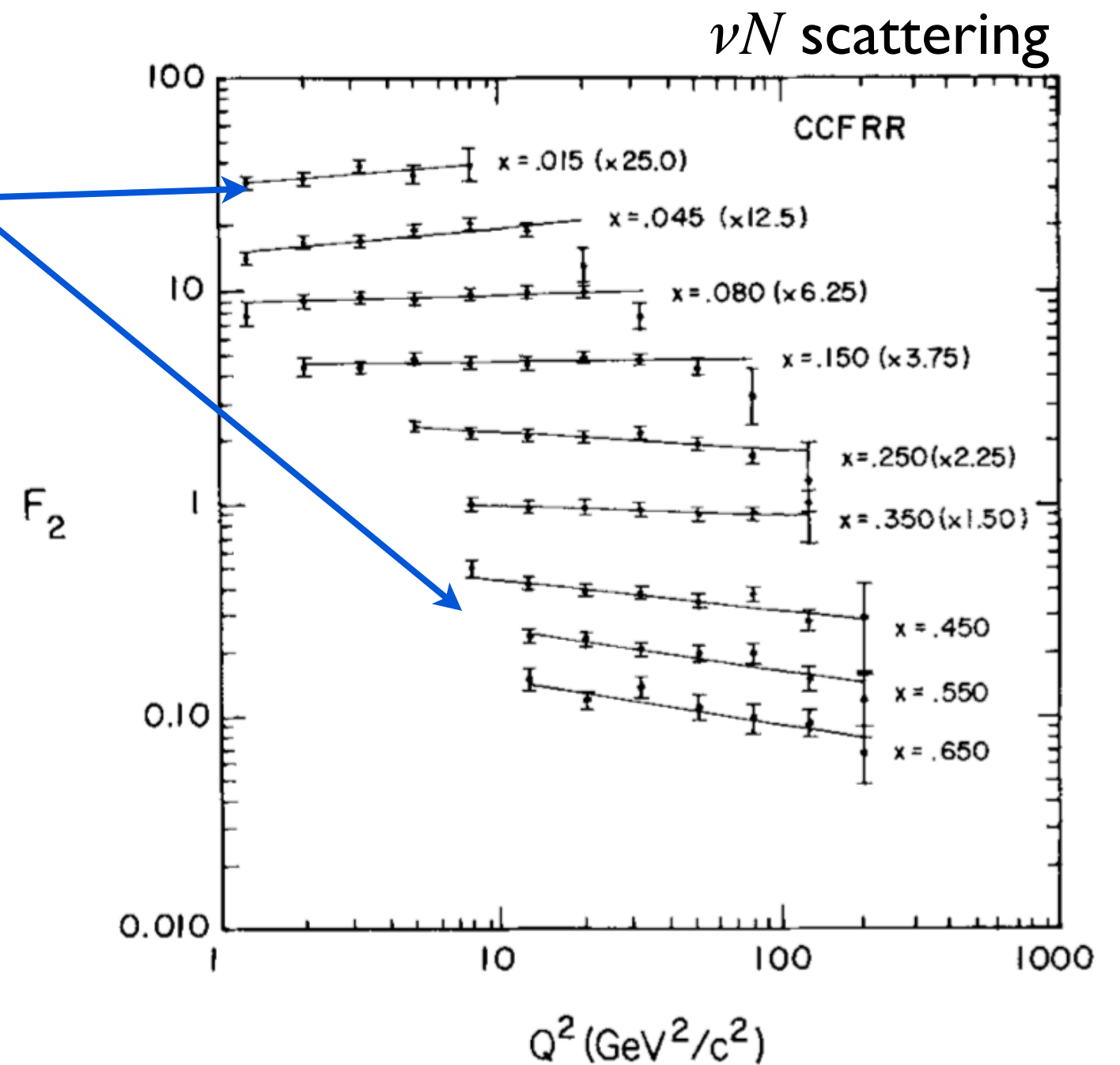
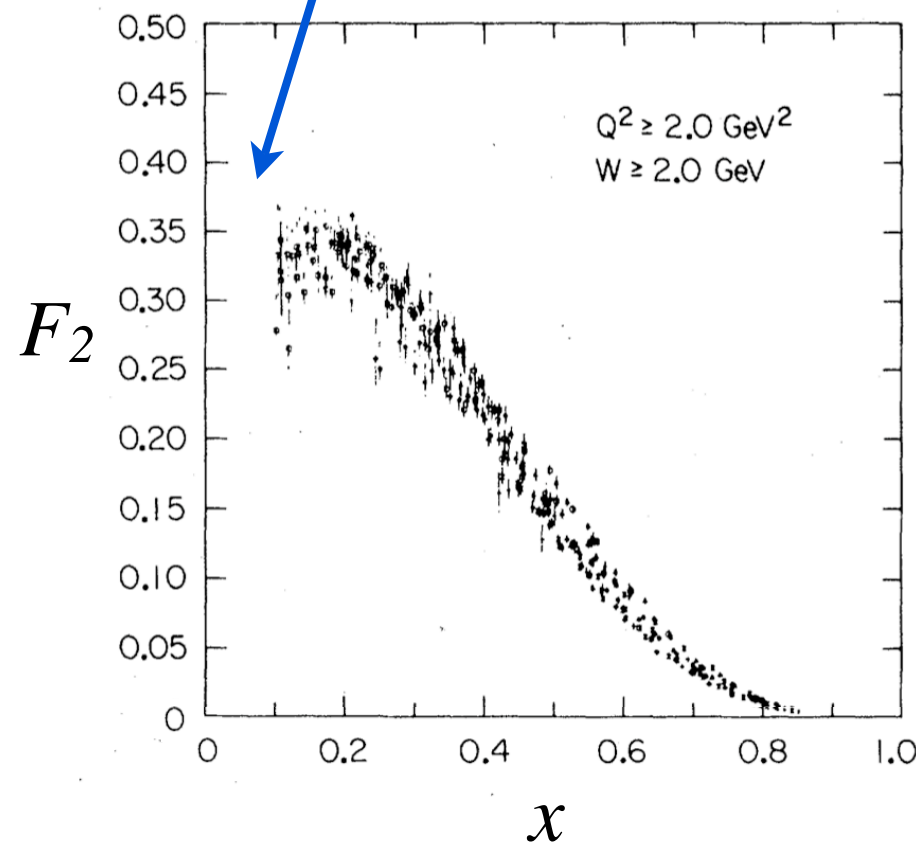
Parton Density Functions

Jet Production

What's Missing?

Is there a Q^2 dependence in F_2 ?

What happens at low x ?

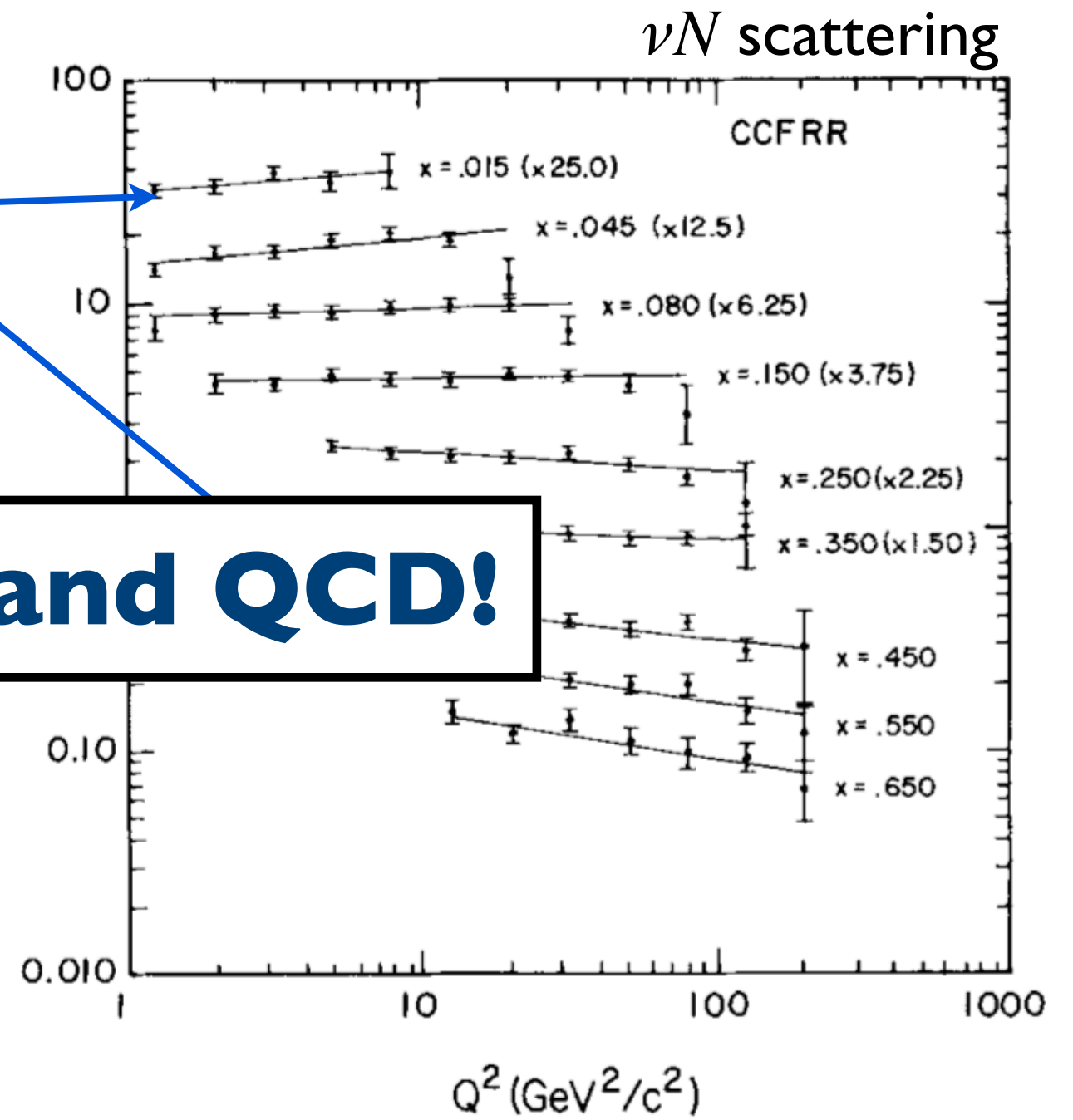
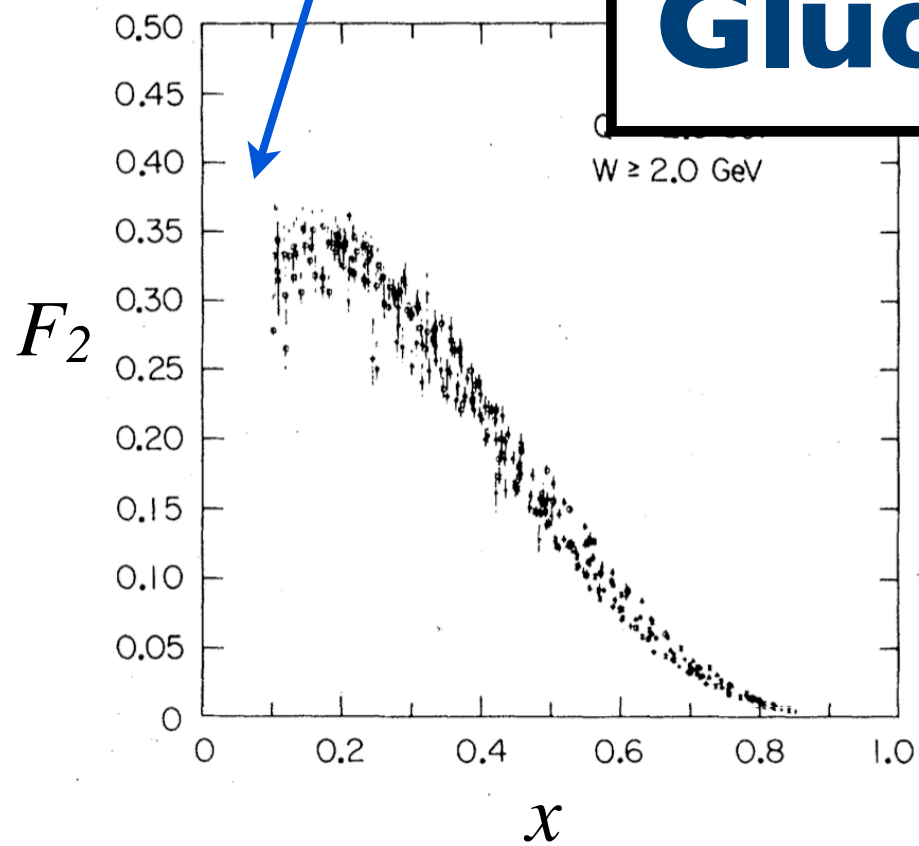


D.B. MacFarlane, et al., Z. Phys. C26, 1 (1984)

What's Missing?

Is there a Q^2 dependence in F_2 ?

What happens at low x ?



Gluons and QCD!

D.B. MacFarlane, et al., Z. Phys. C26, 1 (1984)

QCD

Non-abelian gauge theory with $SU(3)$ symmetry, describes the interaction between coloured particles (quarks and gluons).

The Feynman rules can be derived from the QCD Lagrangian

$$\mathcal{L} = -\frac{1}{4}F_{\mu\nu}^a F_a^{\mu\nu} + \sum_j^{n_f} \bar{q}_j (i\gamma^\mu \mathcal{D}_\mu - m_j) q^j + \mathcal{L}_{\text{gauge}} + \mathcal{L}_{\text{ghost}}$$

Very similar to the QED Lagrangian, except for the additional summation over a , which are the 8 colour degree of freedoms ($SU(3)$ instead of $U(1)$)

Covariant derivative: $\mathcal{D}_\mu = \partial_\mu - ig_s T_a G_\mu^a$

Field strength tensor for spin-1 gluons:

$$F_{\mu\nu}^a = \partial_\mu G_\nu^a - \partial_\nu G_\mu^a - \underbrace{g_s f_{abc} G_\mu^b G_\nu^c}_{\text{Non-abelian term}}$$

Non-abelian term, different from QED. Leads to gluon self-interaction.

The QCD Lagrangian

Let's plug the expressions for \mathcal{D}_μ and $F_{\mu\nu}^a$ into the Lagrangian:

$$\begin{aligned}\mathcal{L} = & \sum_j^{n_f} \bar{q}_j (i\gamma^\mu \partial_\mu - m_q) q^j \\ & - \frac{1}{4} (\partial^\mu G_a^\nu - \partial^\nu G_a^\mu) (\partial_\mu G_\nu^a - \partial_\nu G_\mu^a) \\ & + g_s G_\mu^a \sum_j^{n_f} \bar{q}_j \gamma^\mu T_a q^j \\ & - \frac{g_s}{2} f^{abc} (\partial^\mu G_a^\nu - \partial^\nu G_a^\mu) G_\mu^b G_\nu^c \\ & - \frac{g_s^2}{4} f^{abc} f_{ade} G_b^\mu G_c^\nu G_\mu^d G_\nu^e\end{aligned}$$

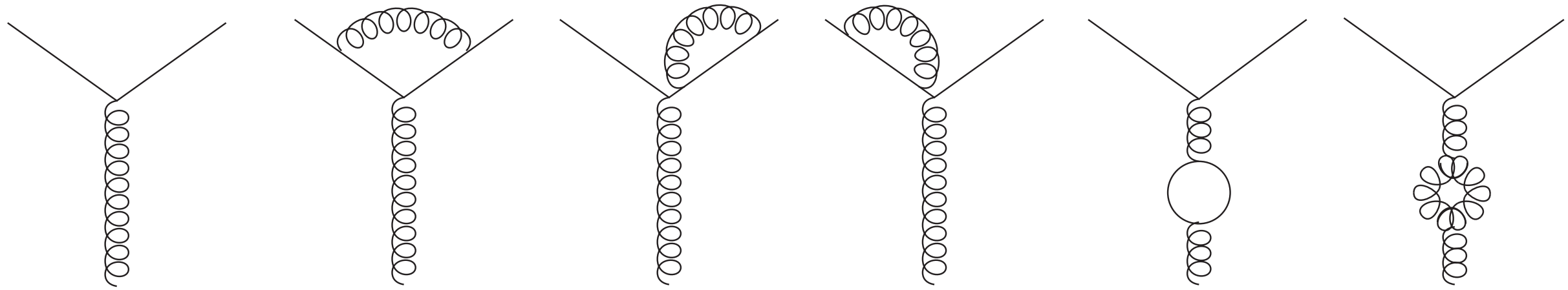
→ [known from QED]

[no QED equivalent]

These terms can then be used to obtain the Feynman rules for QCD

Singularities in QCD

Divergencies appear when constructing the first-order corrections to the quark-gluon interaction



leading order

vertex-correction and
self energies

vacuum polarisation
graphs

finite (?)

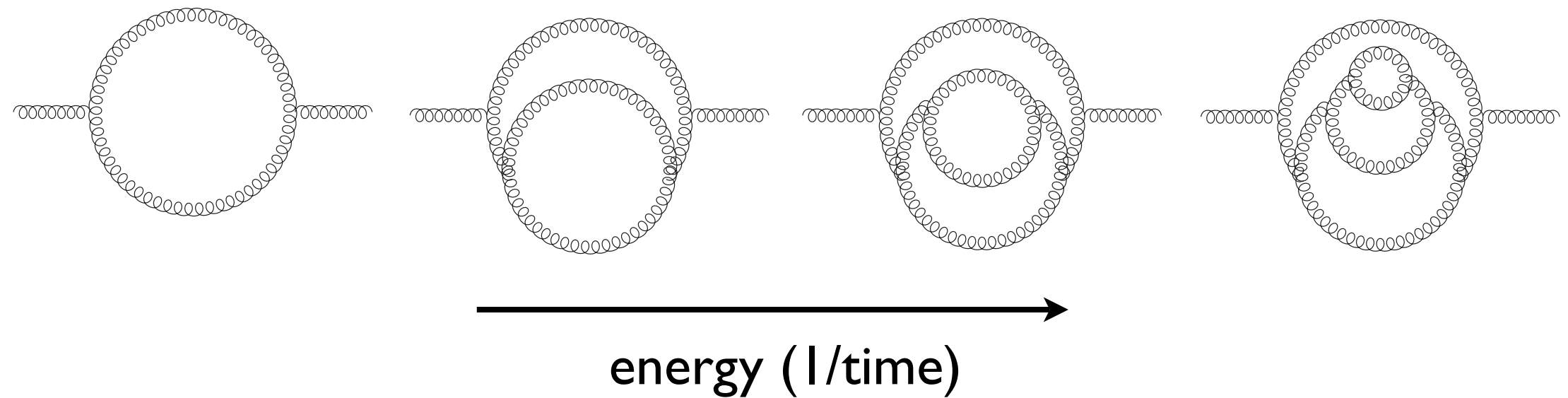
Integrals are infinite, due to unconstraint loop momenta:
ultra-violet (**UV**) divergencies

Known from QED: redefinition of fields and masses will remove the vertex-correction and self energy divergencies (to all orders)

Renormalisation

Ultra-violet (**UV**) divergencies can be interpreted as virtual fluctuations on very small time scales (high energies)

Renormalisation: absorb virtual fluctuations in the definition of the bare coupling, this introduces a new scale parameter μ_R



μ_R has the dimension of energy (mass) and defines the point where the subtraction is performed (ultraviolet cut-off scheme)

More often used but less intuitive: dimensional regularisation, perform integration in $4-2\epsilon$ dimensions

Renormalisation Group Equation

The dimensional parameter μ_R is arbitrary - no general observable $\Gamma(p_i, \alpha_s)$ should depend on it. (strong coupling: $\alpha_s = g_s^2/4\pi$)

Require:
$$\left(\mu_R \frac{\partial}{\partial \mu_R} + \mu_R \frac{\partial \alpha_s}{\partial \mu_R} \frac{\partial}{\partial \alpha_s} + \gamma_\Gamma(\alpha_s) \right) \Gamma(p_i, \alpha_s) = 0$$

Renormalisation Group Equation (RGE)

\Rightarrow a change in μ_R has to be compensated by a change in α_s

Running coupling: $\alpha_s = \alpha_s(\mu_R)$

The quantity $\beta(\alpha_s) = \mu_R \frac{\partial \alpha_s}{\partial \mu_R}$ is known as the QCD beta-function which can be computed.

QCD cannot predict the absolute value of $\alpha_s(\mu_R)$, but its scale dependence.

The Running Coupling

Expansion of the β -function: $\beta(\alpha_s) = -\alpha_s \sum_{n=0}^{\infty} \beta_n \left(\frac{\alpha_s}{4\pi} \right)^{(n+1)}$

Where the terms β_n are known up to four loops:

$$\beta_0 = 11 - \frac{2}{3} n_f$$

$$\beta_1 = 102 - \frac{38}{3} n_f$$

$$\beta_2 = \frac{2857}{2} - \frac{5033}{18} n_f + \frac{325}{54} n_f^2$$

$$\beta_3 = \frac{149753}{6} + 3564\zeta_3 - \left(\frac{1078361}{162} + \frac{6508}{27} \zeta_3 \right) n_f$$

$$+ \left(\frac{50065}{162} + \frac{6472}{81} \zeta_3 \right) n_f^2 + \frac{1093}{729} n_f^3$$

In Fact...

$$\frac{\partial a_s}{\partial \ln \mu_R} = -\beta_0 a_s^2 - \beta_1 a_s^3 - \beta_2 a_s^4 - \beta_3 a_s^5 + \mathcal{O}(a_s^6) \quad (a_s = \alpha_s/4\pi)$$

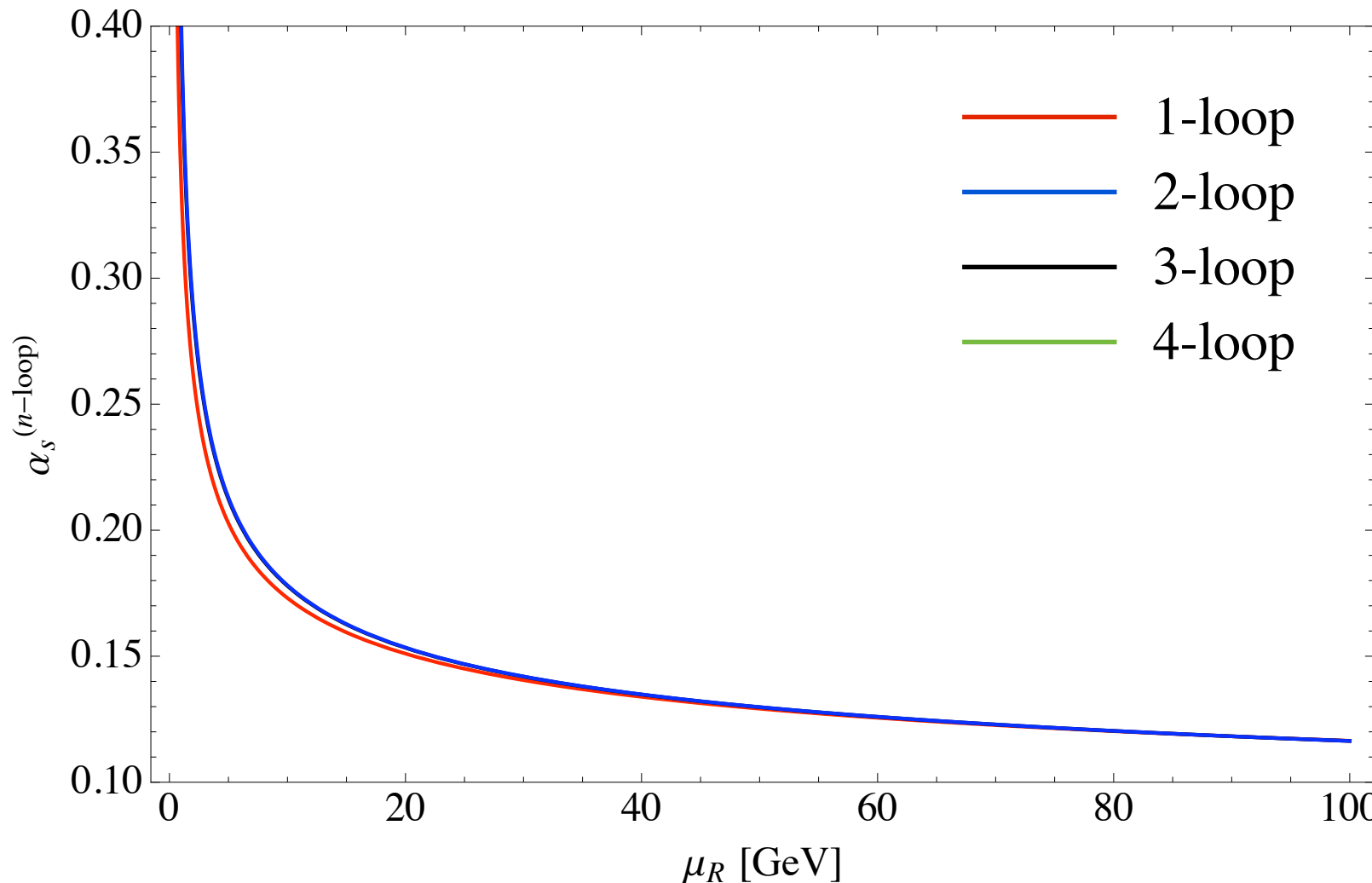
$$\begin{aligned}
 \beta_0 &= \frac{11}{3}C_A - \frac{4}{3}T_F n_f, \quad \beta_1 = \frac{34}{3}C_A^2 - 4C_F T_F n_f - \frac{20}{3}C_A T_F n_f \\
 \beta_2 &= \frac{2857}{54}C_A^3 + 2C_F^2 T_F n_f - \frac{205}{9}C_F C_A T_F n_f \\
 &\quad - \frac{1415}{27}C_A^2 T_F n_f + \frac{44}{9}C_F T_F^2 n_f^2 + \frac{158}{27}C_A T_F^2 n_f^2 \\
 \beta_3 &= C_A^4 \left(\frac{150653}{486} - \frac{44}{9}\zeta_3 \right) + C_A^3 T_F n_f \left(-\frac{39143}{81} + \frac{136}{3}\zeta_3 \right) \\
 &\quad + C_A^2 C_F T_F n_f \left(\frac{7073}{243} - \frac{656}{9}\zeta_3 \right) + C_A C_F^2 T_F n_f \left(-\frac{4204}{27} + \frac{352}{9}\zeta_3 \right) \\
 &\quad + 46C_F^3 T_F n_f + C_A^2 T_F^2 n_f^2 \left(\frac{7930}{81} + \frac{224}{9}\zeta_3 \right) + C_F^2 T_F^2 n_f^2 \left(\frac{1352}{27} - \frac{704}{9}\zeta_3 \right) \\
 &\quad + C_A C_F T_F^2 n_f^2 \left(\frac{17152}{243} + \frac{448}{9}\zeta_3 \right) + \frac{424}{243}C_A T_F^3 n_f^3 + \frac{1232}{243}C_F T_F^3 n_f^3 \\
 &\quad + \frac{d_A^{abcd} d_A^{abcd}}{N_A} \left(-\frac{80}{9} + \frac{704}{3}\zeta_3 \right) + n_f \frac{d_F^{abcd} d_A^{abcd}}{N_A} \left(\frac{512}{9} - \frac{1664}{3}\zeta_3 \right) \\
 &\quad + n_f^2 \frac{d_F^{abcd} d_F^{abcd}}{N_A} \left(-\frac{704}{9} + \frac{512}{3}\zeta_3 \right)
 \end{aligned}$$

evaluation of
~ 50 000 diagrams

T. van Ritbergen, et al., Phys. Lett. B400, 379 (1997)



The Running Coupling in QCD



Asymptotically free
for $\mu_R \rightarrow \infty$

Good convergence
(expansion parameter
 $a_s \approx 0.01$)

No visible difference
between 3-loop and
4-loop solution

The scale dependence $\alpha_s(\mu_R)$ of is one of the best known quantities in QCD

⇒ Possibility for stringent tests of QCD!

Another Challenge

The small values of $\alpha_s(\mu_R)$ at large scales allows the application of perturbation theory

But as $\mu_R \rightarrow 0$, $\alpha_s(\mu_R)$ becomes large and higher order corrections become increasingly important \Rightarrow diagram techniques fail for bound states in QCD

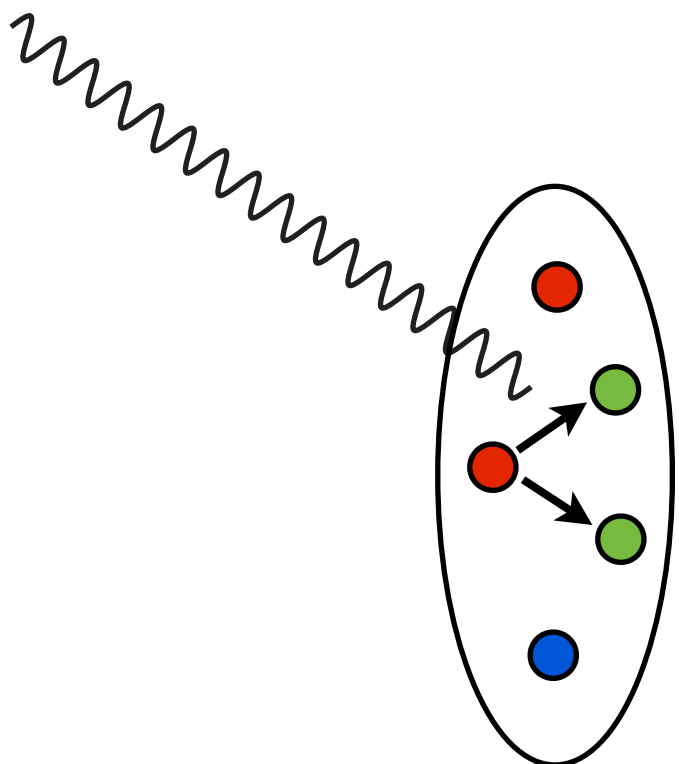
How can we calculate anything with hadrons in the initial / final state involved?

Another Challenge

The small values of $\alpha_s(\mu_R)$ at large scales allows the application of perturbation theory

But as $\mu_R \rightarrow 0$, $\alpha_s(\mu_R)$ becomes large and higher order corrections become increasingly important \Rightarrow diagram techniques fail for bound states in QCD

How can we calculate anything with hadrons in the initial / final state involved?



Answer: different time / length scales!

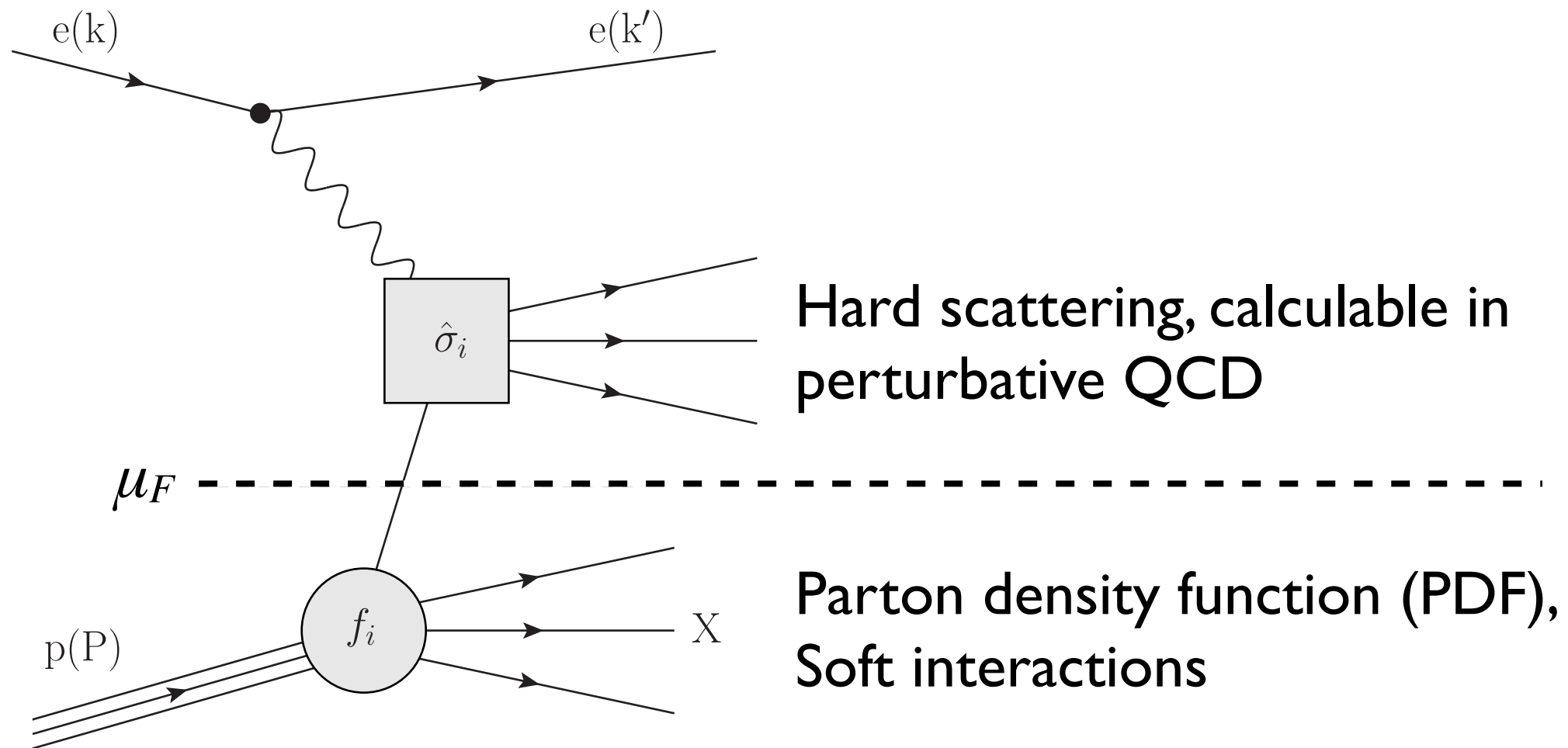
Timescale of proton fluctuation: $t = \frac{1}{\Delta E} \approx \frac{k_T^2}{2xP}$

Timescale of interaction: $\tau = \frac{1}{E_\gamma} = \frac{2xP}{Q^2}$

$\frac{t}{\tau} \approx \frac{k_T^2}{Q^2} \ll 1$ proton is ‘frozen’ during the interaction

Factorisation

Absorb long time (small scale) effects in the proton structure



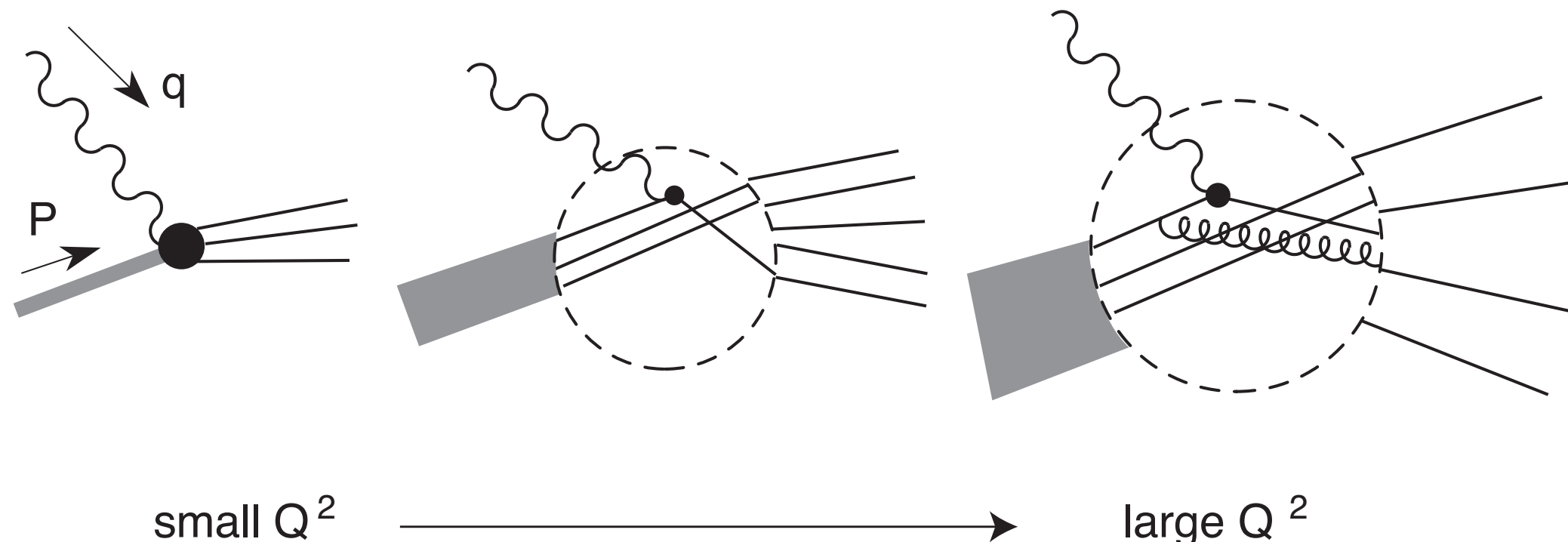
The factorisation scale μ_F gives the separation between long and short time physics

- PDFs acquire a scale dependence
- PDFs can not be predicted by QCD

Parton Evolution

Intuitive picture: the number of partons changes with scale $\mu_F = Q^2$

The virtual photon as probe with resolving power $Q^2 \sim 1 / \lambda$



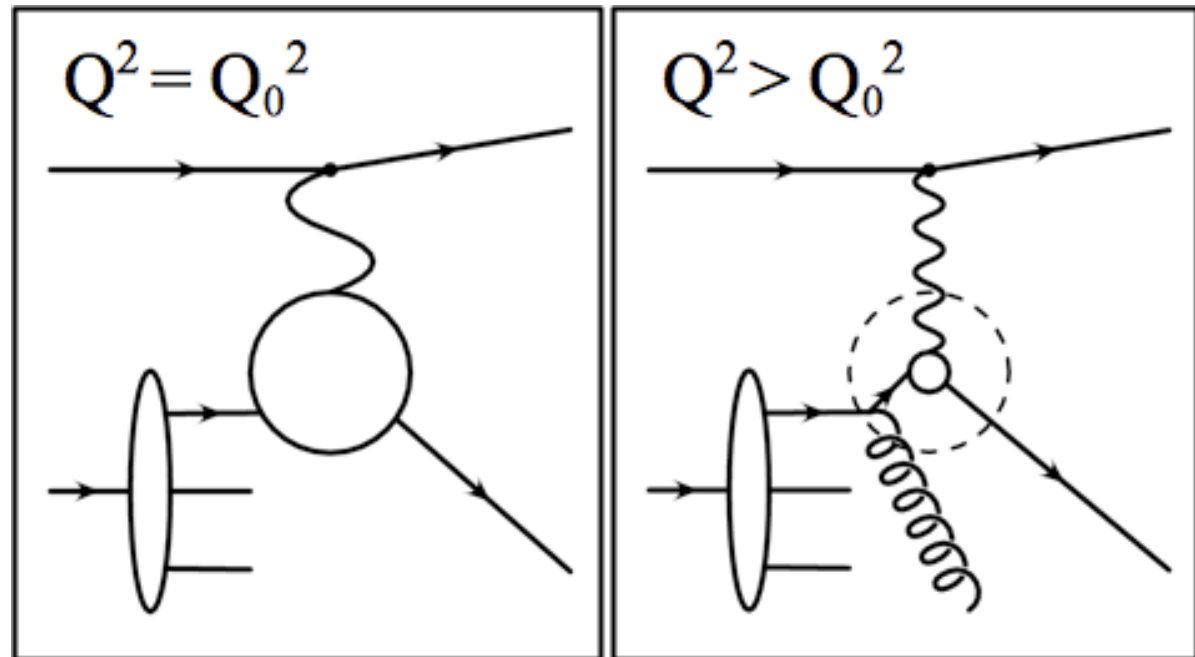
many partons with large x

we 'see' parton radiation, branchings
⇒ many partons with small x

Drawing from A. Pich, arXiv:hep-ph/9505231 (1995)

Scaling Violations

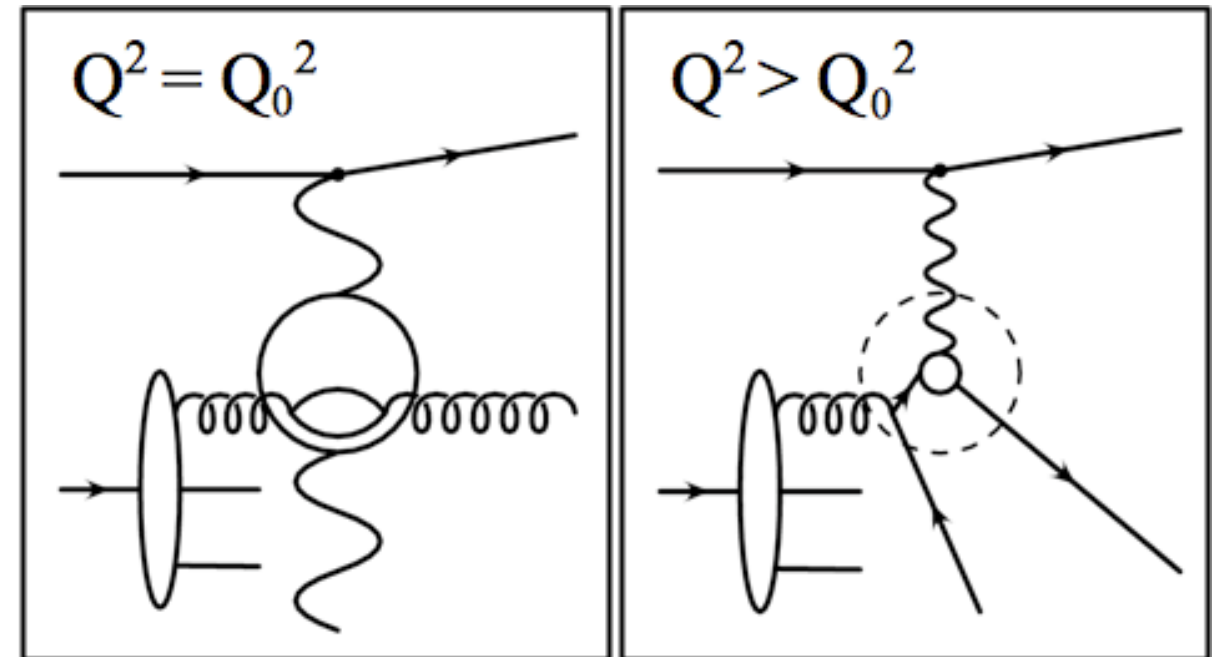
Large x



With increasing Q^2 , the valence quarks radiate more and more gluons, so the studied x decreases

F_2 decreases with increasing Q^2

Small x



Gluons split into sea quarks, which can be resolved with increasing Q^2 , more quarks become visible

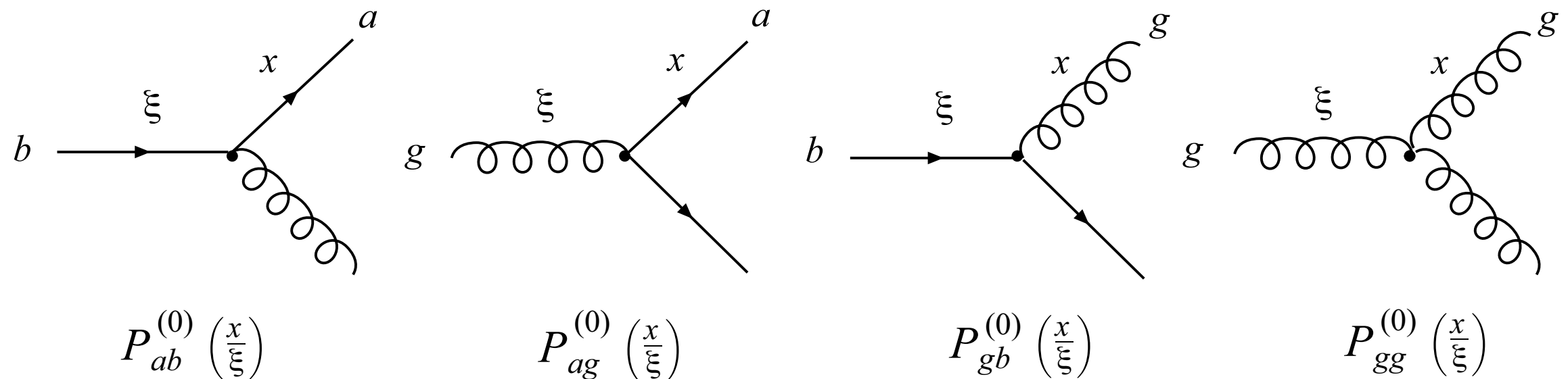
F_2 increases with increasing Q^2

DGLAP Equations

It is possible to calculate the evolution of partons in QCD:
DGLAP equations (Dokshitzer-Gribov-Lipatov-Altarelli-Parisi)

$$\frac{\partial}{\partial \ln \mu_F^2} \begin{pmatrix} q_i(x, \mu_F^2) \\ g(x, \mu_F^2) \end{pmatrix} = \frac{\alpha_s(\mu_R)}{2\pi} \sum_j \int_x^1 \frac{d\xi}{\xi} \begin{pmatrix} P_{q_i q_j}(\frac{x}{\xi}) & P_{q_i g}(\frac{x}{\xi}) \\ P_{g q_j}(\frac{x}{\xi}) & P_{g g}(\frac{x}{\xi}) \end{pmatrix} \begin{pmatrix} q_j(\xi, \mu_F^2) \\ g(\xi, \mu_F^2) \end{pmatrix}$$

Splitting functions $P_{ab}(x/\xi)$: meaning (in LO) of an emission probability:



We can predict the scale dependence of the quark $q(x, \mu_F)$ and gluon $g(x, \mu_F)$ distributions!

F₂ Revisited

In the QPM we had: $F_2(x) = x \sum_i e_i^2 q_i(x)$

Now we have ($\overline{\text{MS}}$ -scheme used) (in DIS use $\mu_F = Q^2$)

$$\begin{aligned} F_2(x, Q^2) &= x \sum_{q, \bar{q}} e_q^2 \int_x^1 \frac{d\xi}{\xi} q(\xi, Q^2) \left[\delta \left(1 - \frac{x}{\xi} \right) + \frac{\alpha_s}{2\pi} C_q^{\overline{\text{MS}}} \left(\frac{x}{\xi} \right) + \dots \right] \\ &+ x \sum_{q, \bar{q}} e_q^2 \int_x^1 \frac{d\xi}{\xi} g(\xi, Q^2) \left[\frac{\alpha_s}{2\pi} C_g^{\overline{\text{MS}}} \left(\frac{x}{\xi} \right) + \dots \right] \end{aligned}$$

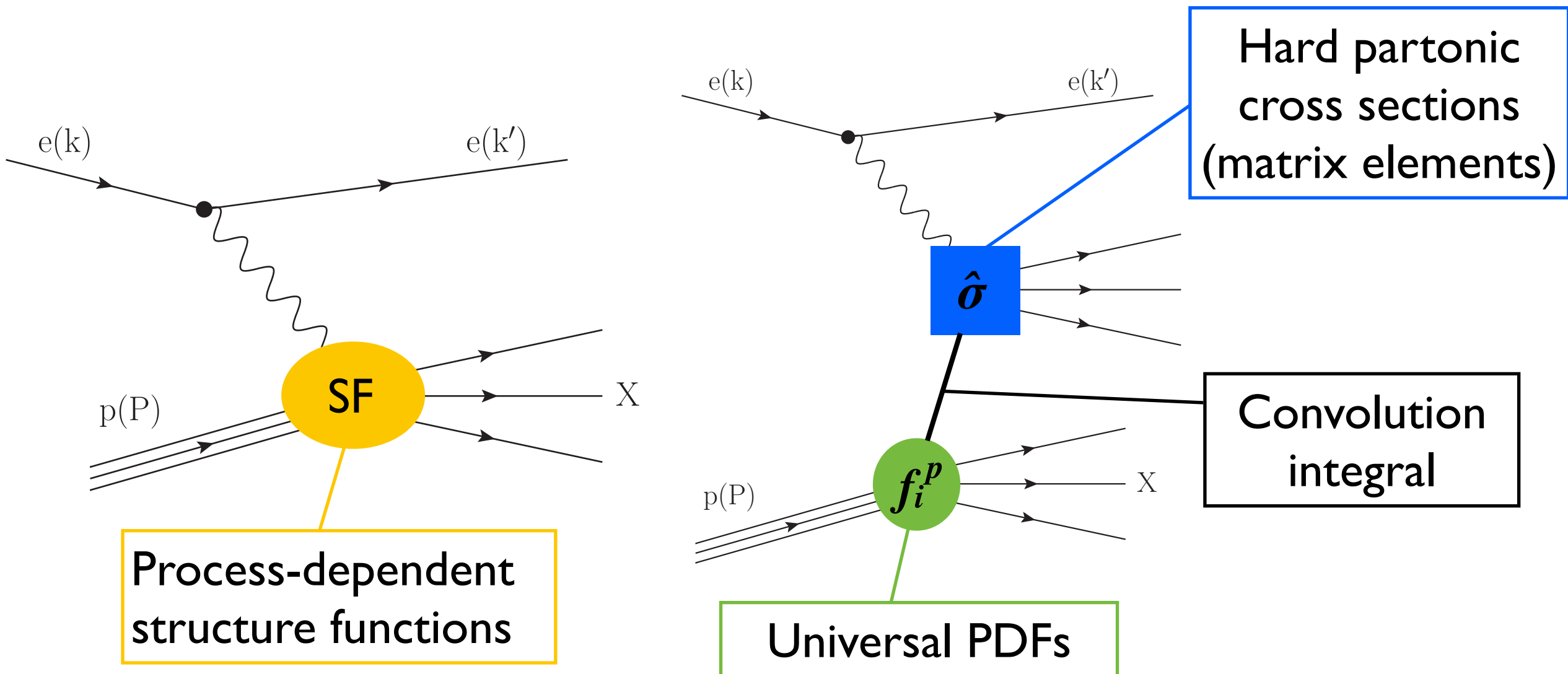
($C_q^{\overline{\text{MS}}}$ and $C_g^{\overline{\text{MS}}}$ are scheme-dependent coefficient functions)

- In leading order (LO) we get back to the QPM
- F_2 obtained an explicit Q^2 dependence
- In next-to-leading order (NLO) F_2 is sensitive to the gluon component

Structure Functions and PDFs

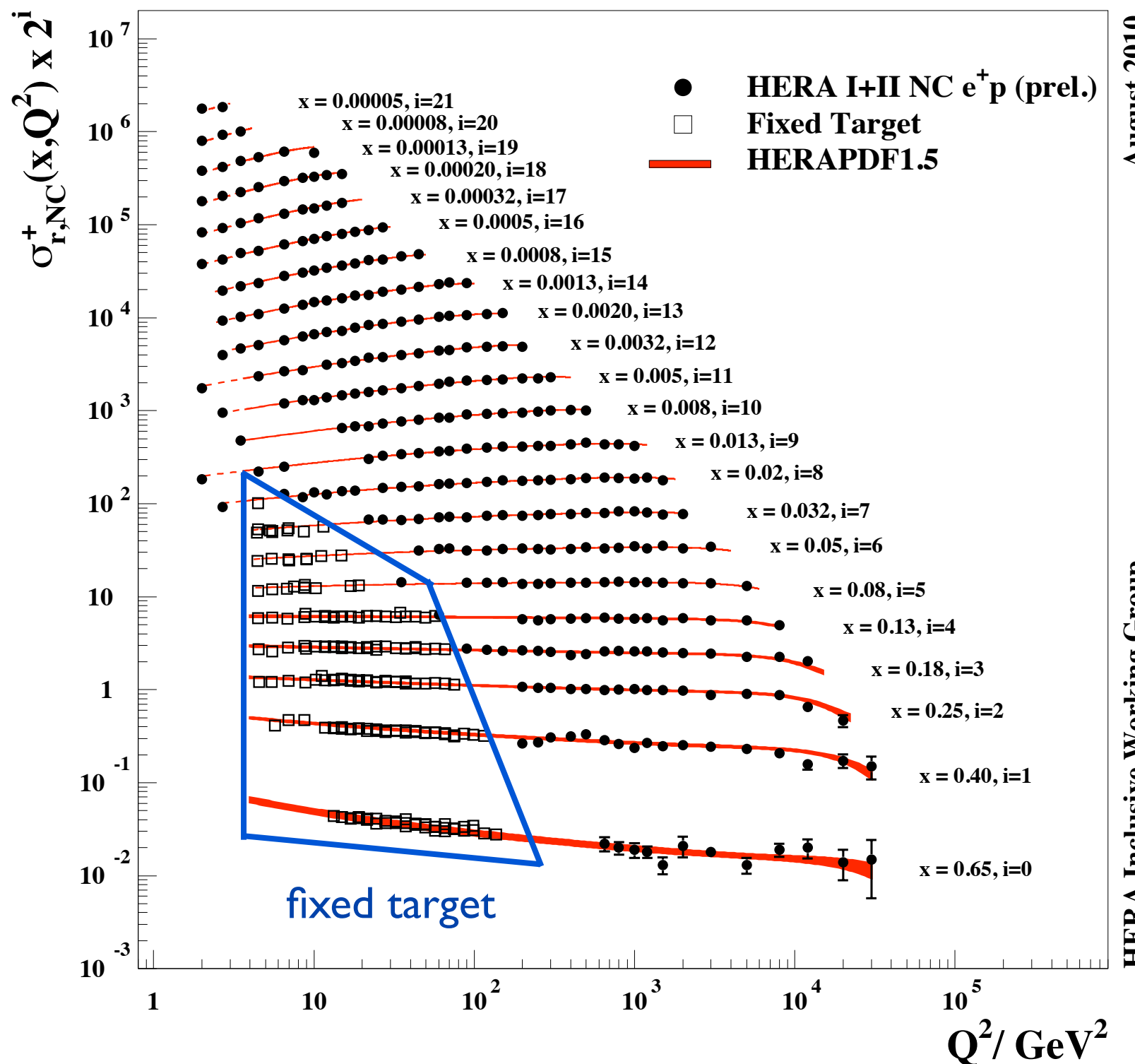
A common misconception:

Parton Distribution Functions \neq Structure Functions



F₂ From HERA

H1 and ZEUS



August 2010
HERA Inclusive Working Group

$$\sigma_{r,NC}^+(x, Q^2) = \frac{d^2\sigma_{NC}^{e^+p}}{dQ^2 dx} \frac{xQ^4}{2\pi\alpha^2 Y_+} \approx F_2(x, Q^2)$$

HERA data cover 5 orders in Q^2 and 4 orders in x

Approximate scaling at intermediate x

Clear scaling violations at small and large x

DGLAP works!
Huge success of QCD

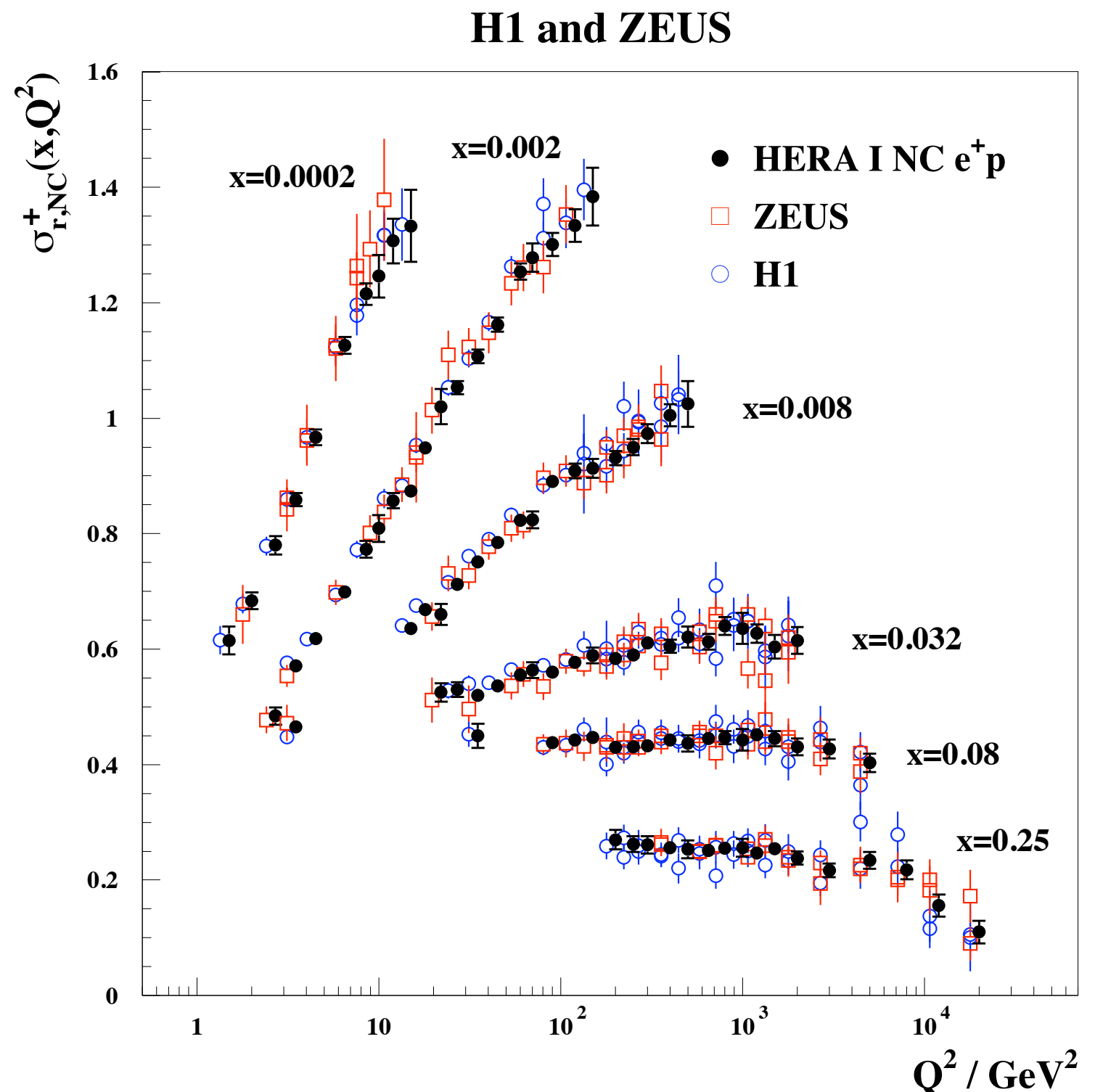


F_2 From H1 and ZEUS: Combination

Scaling violations on a linear scale, some example regions

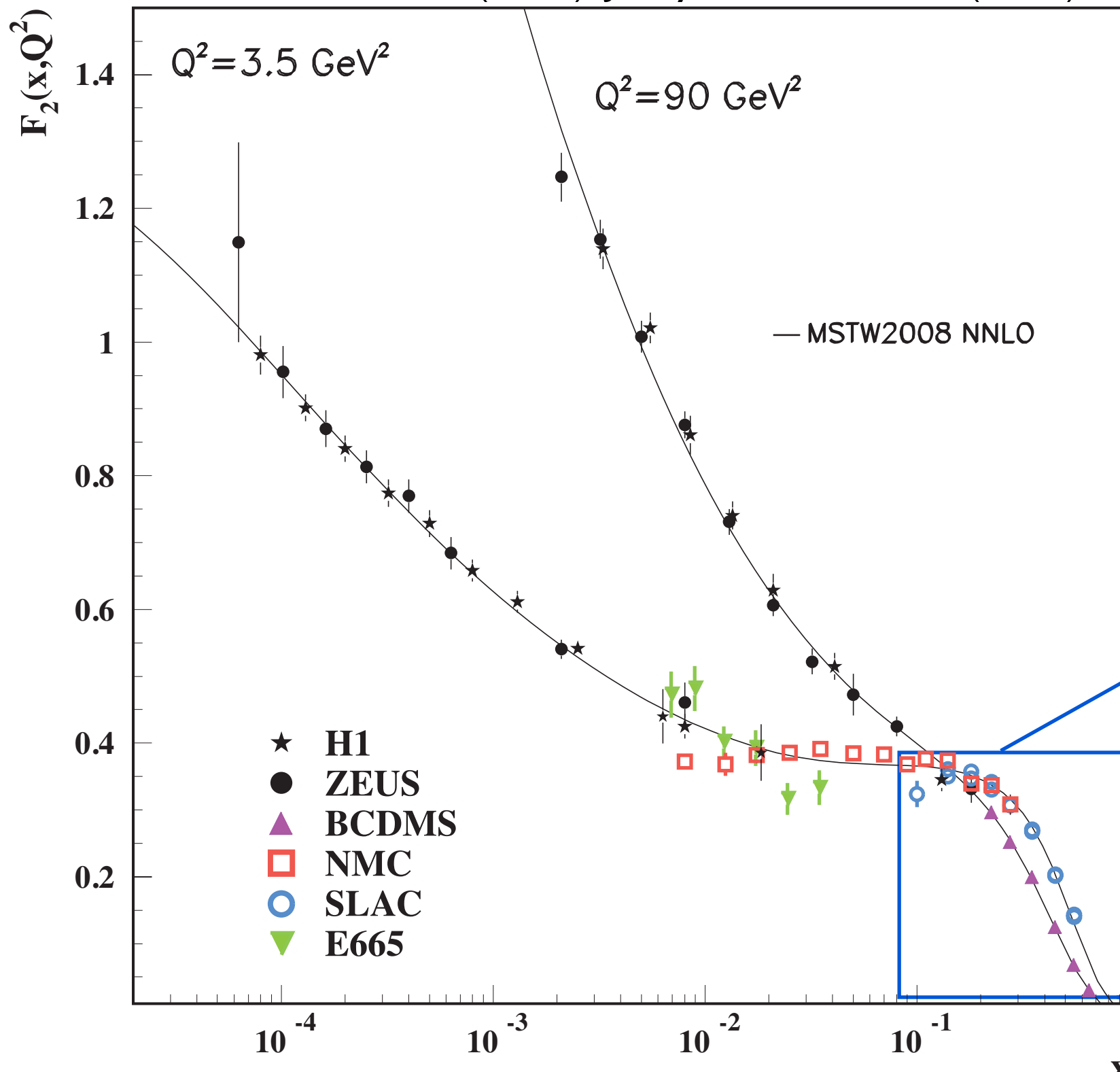
Combination of H1 and ZEUS data

- improved statistics
- cross-calibration helps to reduce the systematic uncertainty



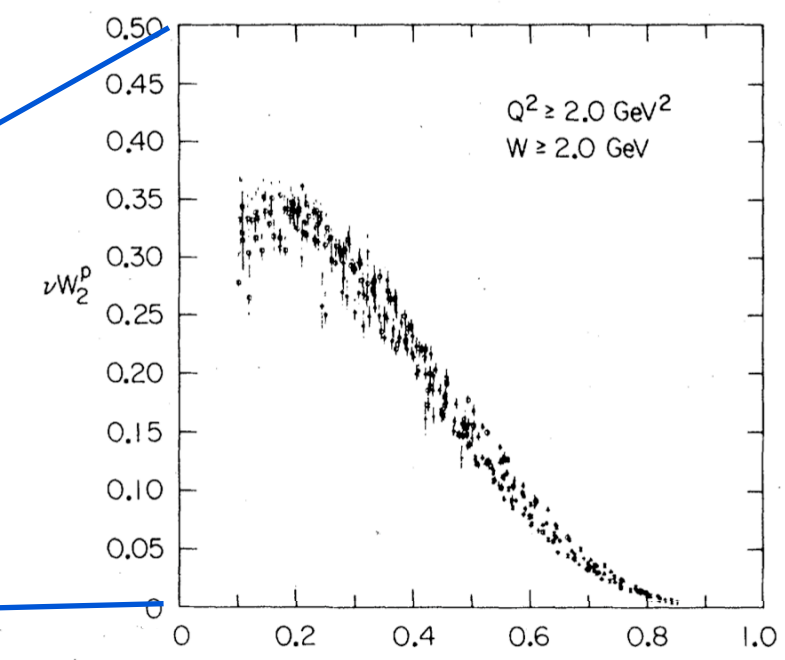
What Happens At Low x ?

K. Nakamura, et al. (PDG), J. Phys. G37, 075021 (2010)



Early HERA data compared to fixed-target experiments

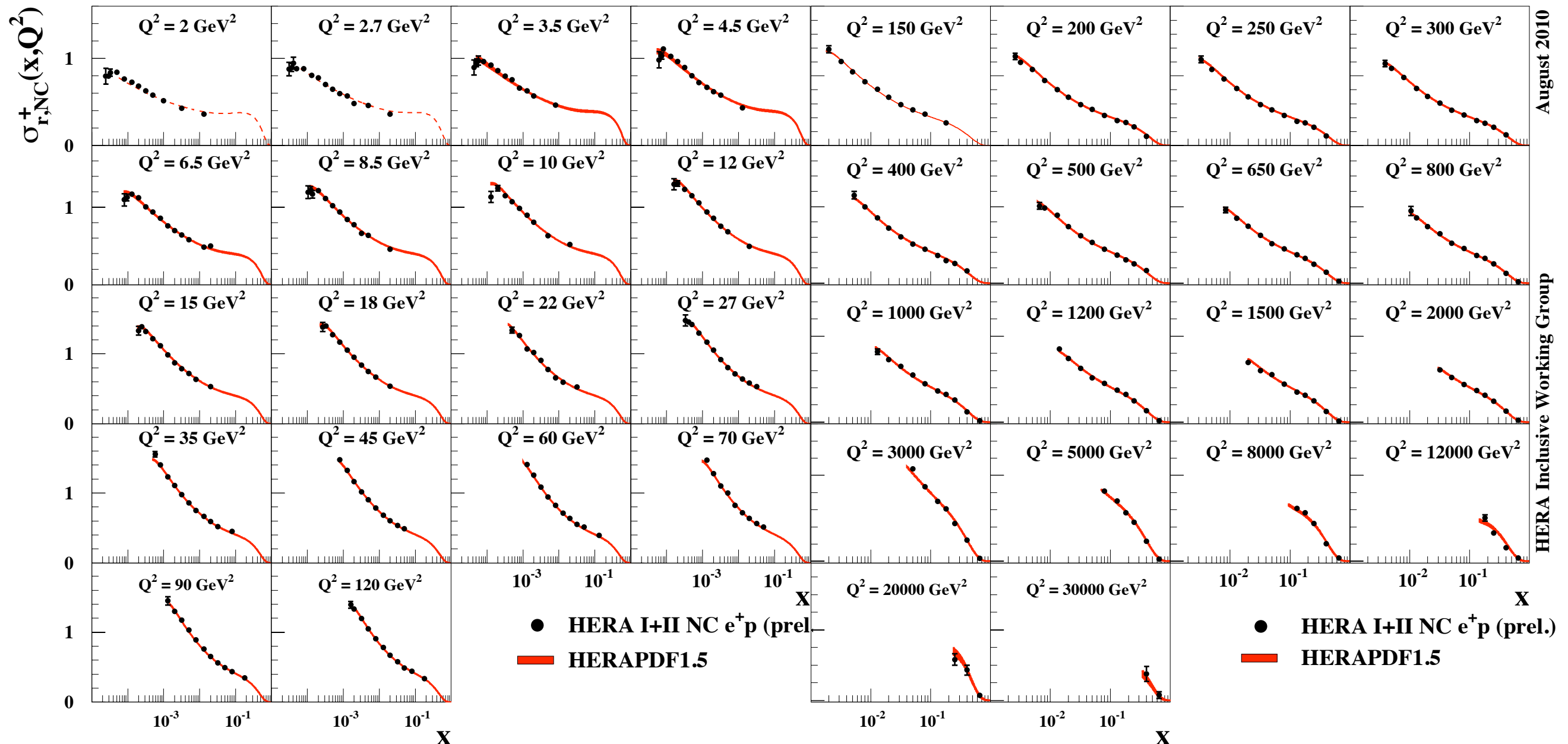
Strong rise of F_2 towards small x , becoming steeper with increasing Q^2



Strong Rise Of F_2 Versus x

H1 and ZEUS

H1 and ZEUS



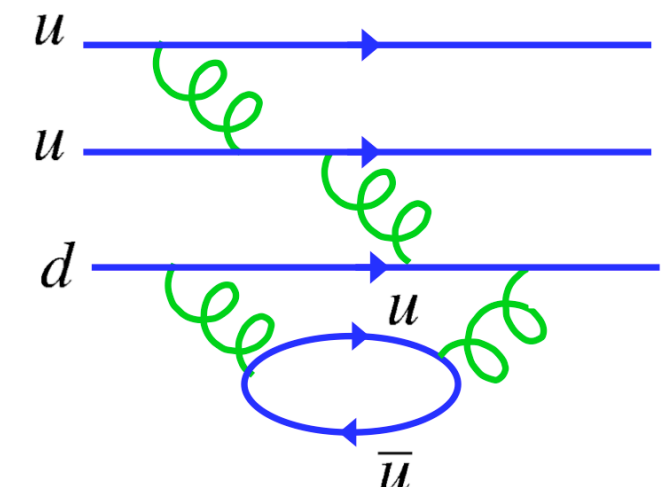
Strong rise of F_2 towards small x , becoming steeper with increasing Q^2

Parton Distribution Functions (PDFs)

Modify the simple QPM picture, where the proton was only made up of two up and one down quark

The up- and down-quark distributions obtain contributions from the **valence** quarks and the virtual **sea** quarks

$$u(x) = u_v(x) + u_s(x) \text{ and } d(x) = d_v(x) + d_s(x)$$



anti-quarks originate only from the sea

$$\bar{u}(x) = \bar{u}_s(x) \text{ and } \bar{d}(x) = \bar{d}_s(x)$$

The proton consists of two up quarks and one down quark:

$$\int_0^1 u_v(x) dx = 2 \text{ and } \int_0^1 d_v(x) dx = 1 \quad (\text{quark number sum rules})$$

No a-priori expectation for the number of sea quarks and gluons.

Constituents Of The Proton

In general we have 10 quark and anti-quark densities and the gluon:

$$u, \bar{u}, d, \bar{d}, s, \bar{s}, c, \bar{c}, (b, \bar{b}), g$$

Distinguish only between up-type and down-type quarks:

$$\begin{aligned} U &= u (+ c), \quad D = d + s (+ b) \\ \bar{U} &= \bar{u} (+ \bar{c}), \quad \bar{D} = \bar{d} + \bar{s} (+ \bar{b}) \end{aligned}$$

Then the valence quark distributions are

$$u_v = U - \bar{U}, \quad d_v = D - \bar{D}$$

The total sea distribution is often expressed as

$$S = 2(\bar{U} + \bar{D})$$

and the **momentum sum rule** has to be fulfilled

$$\int_0^1 \left[\sum_i (q_i(x) + \bar{q}_i(x)) + g(x) \right] x dx = 1$$



From F_2 To PDFs

QCD (DGLAP) predicts scale dependence of quark and gluon densities

x-dependence can not be calculated in perturbative QCD
(reminder: renormalisation of the bare quark and gluon densities -
soft, long-range effects are absorbed in the PDF)

Need to obtain the x-dependence from experiment!

- › Parametrise $q_i(x), g(x)$ at a starting scale Q_0
- › Use DGLAP to evolve F_2 to a higher scale (and calculate $\sigma_r(x, Q^2)$)
- › Determine the parameters from a fit to data

Note: Q_0^2 has to be smaller than the lowest value of Q^2 in the data

Only limited number of free parameters possible

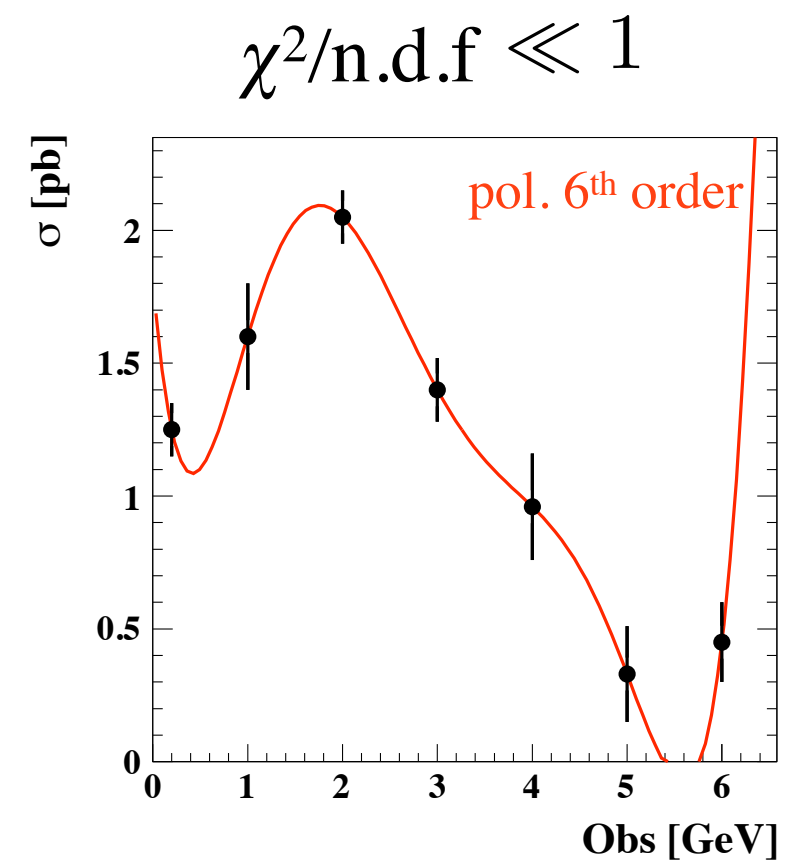
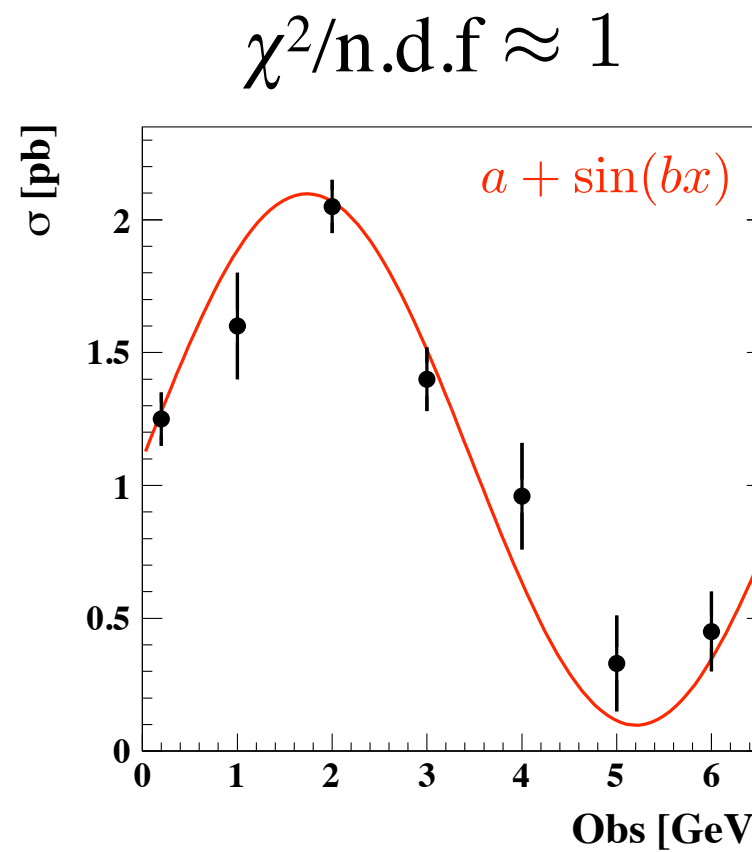
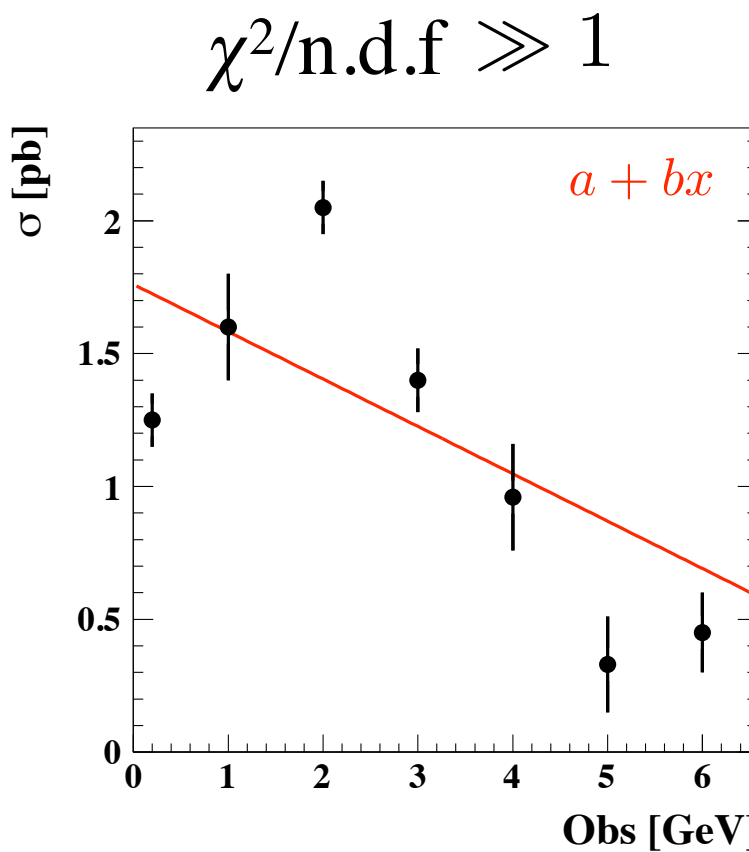
Use physical constraints for PDFs

A Note On Fits

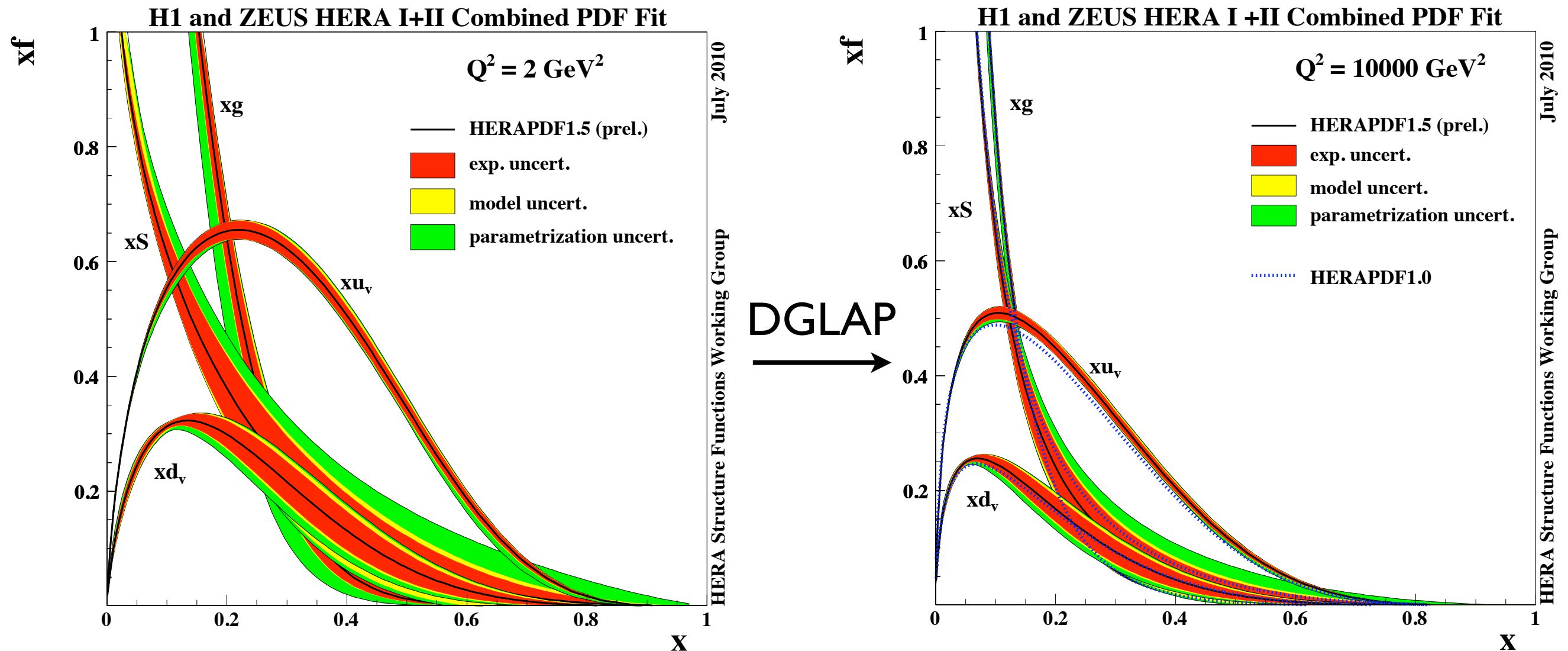
Fit (in physics): ‘Minimise the difference between data and theoretical predictions by adjusting free parameters.’

Quantify the difference with a single variable: $\chi^2(d, t(x))$

Naïve definition: $\chi^2 = \sum_i \frac{(d_i - t_i(x))^2}{\sigma_i^2}$



HERAPDF



10 free parameters, about 1000 data points entered the fit, $\chi^2/\text{n.d.f} \approx 0.94$

$u_v \approx 2d_v$, gluon starts to dominate around $x \sim 0.2$

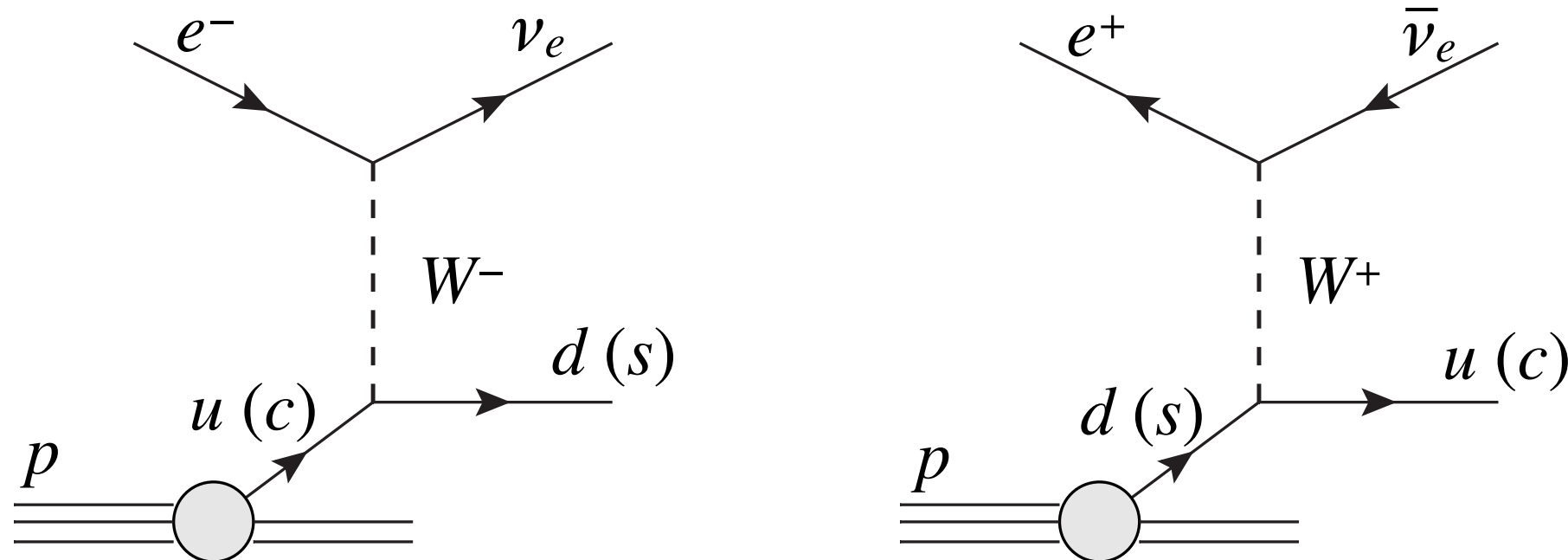
Disentangling u_ν From d_ν

In the extraction of PDFs, how can we distinguish between u_ν and d_ν ?

Disentangling u_ν From d_ν

In the extraction of PDFs, how can we distinguish between u_ν and d_ν ?

Charged Current Interactions

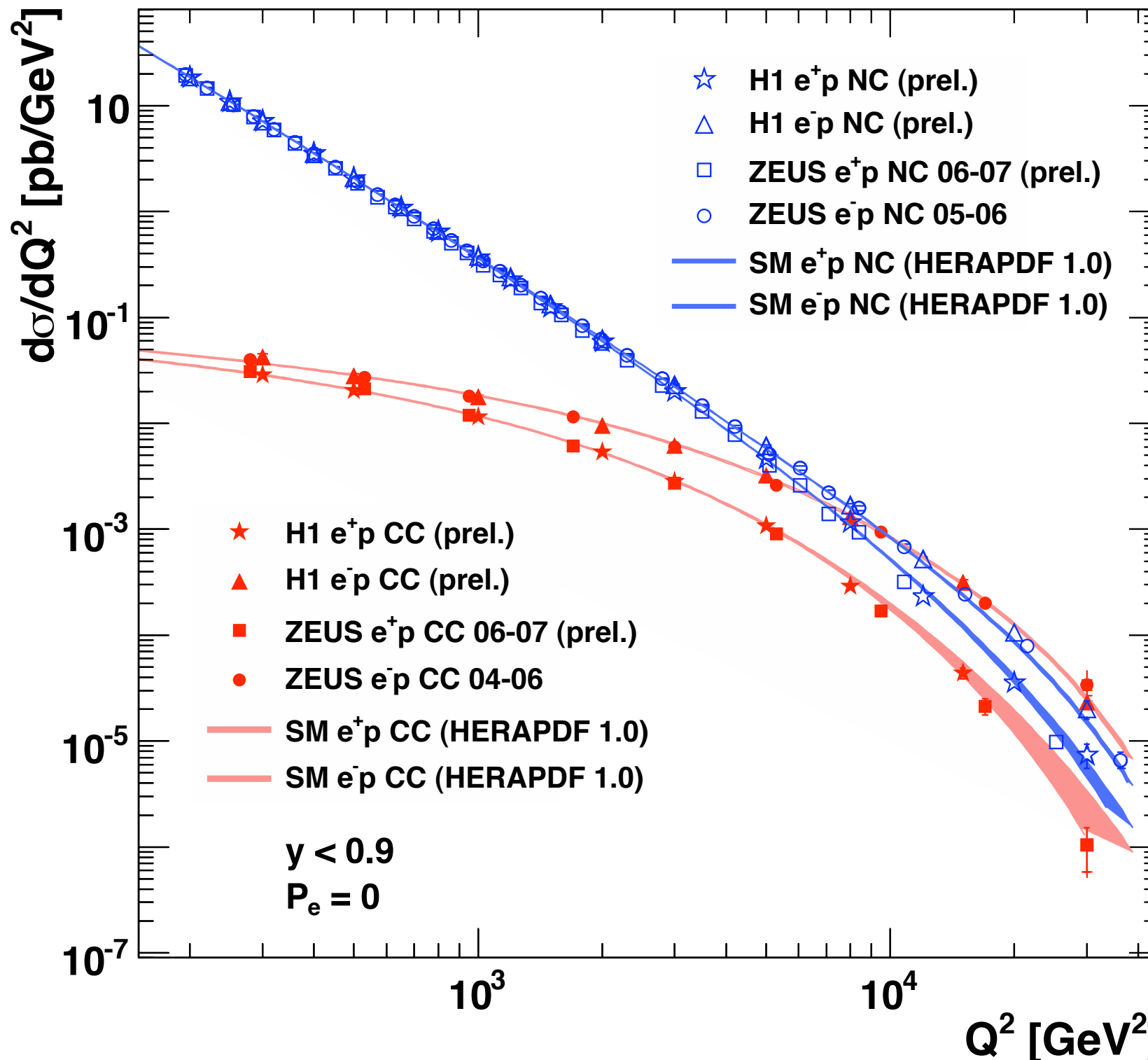


$$\frac{d^2\sigma_{CC}^-}{dx dQ^2} = \frac{G_F^2}{2\pi} \left(\frac{M_W^2}{M_W^2 + Q^2} \right)^2 [u(x) + c(x) + (1 - y)^2(\bar{d}(x) + \bar{s}(x))]$$

$$\frac{d^2\sigma_{CC}^+}{dx dQ^2} = \frac{G_F^2}{2\pi} \left(\frac{M_W^2}{M_W^2 + Q^2} \right)^2 [\bar{u}(x) + \bar{c}(x) + (1 - y)^2(d(x) + s(x))]$$

The NC and CC Cross Sections

HERA



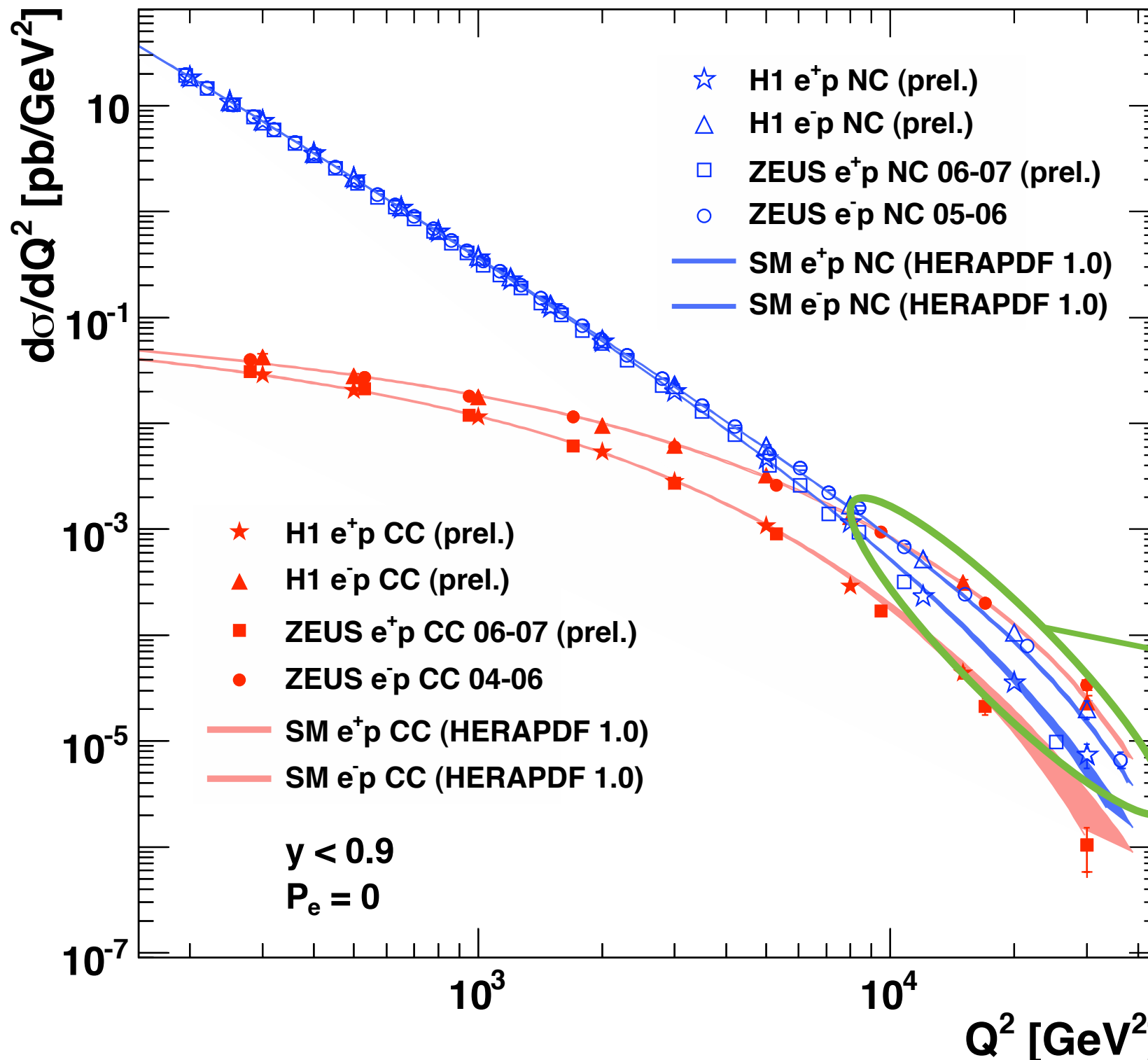
NC and CC cross sections become comparable at

$$Q^2 \approx M_W^2 \approx 6500 \text{ GeV}^2$$

$e^+p \rightarrow \bar{\nu}_e + X$ cross section only half as big as $e^-p \rightarrow \nu_e + X$

The NC and CC Cross Sections

HERA



NC and CC cross sections become comparable at

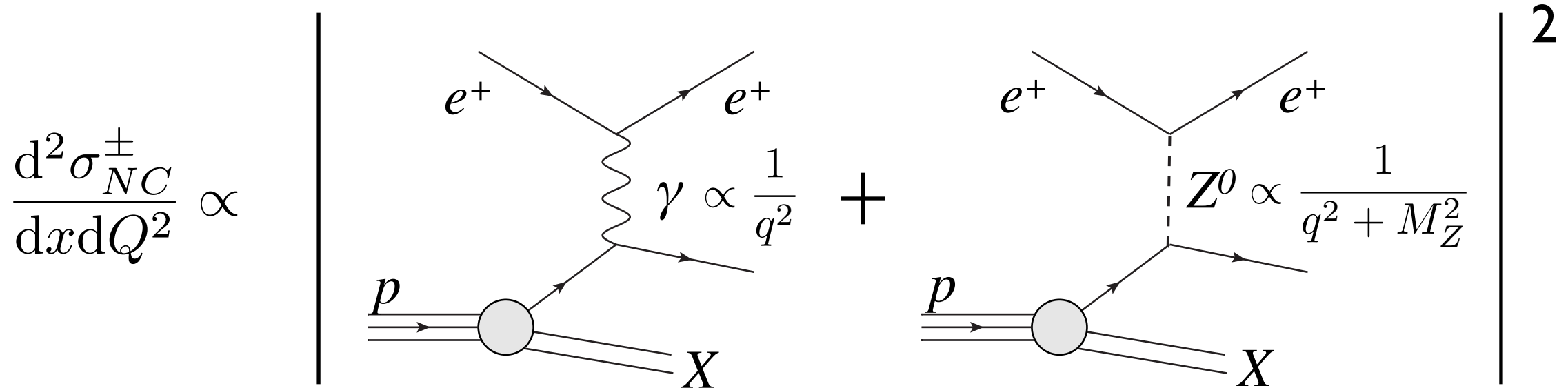
$$Q^2 \approx M_W^2 \approx 6500 \text{ GeV}^2$$

$e^+p \rightarrow \bar{\nu}_e + X$ cross section only half as big as $e^-p \rightarrow \nu_e + X$

Why is there a difference in the NC cross sections for e^+p and e^-p scattering?

Z⁰ Exchange

At $Q^2 \approx M_Z^2$ effects from Z^0 exchange cannot be neglected anymore



$$\frac{d^2\sigma_{NC}^\pm}{dx dQ^2} = \frac{2\pi\alpha^2}{Q^4 x} [Y_+ \underline{F_2(x, Q^2)} \mp Y_- \underline{x F_3(x, Q^2)}] \quad (Y_\pm = 1 \pm (1 - y)^2)$$

$$F_2(x, Q^2) = F_2^\gamma - a_{\gamma Z} \kappa_Z F_2^{\gamma Z} + a_Z \kappa_Z^2 F_2^Z$$

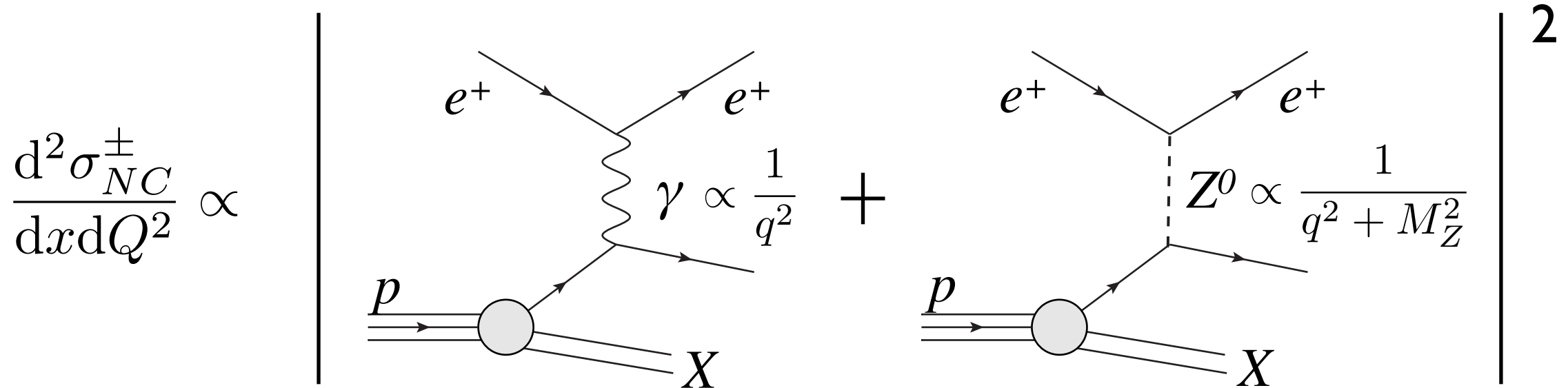
$$\kappa_Z = \frac{Q^2}{Q^2 + M_Z^2} \frac{1}{\sin^2 2\theta_W}$$

$$x F_3(x, Q^2) = -x b_{\gamma Z} \kappa_Z F_3^{\gamma Z} + x b_Z \kappa_Z^2 F_3^Z$$

Parity violating structure function

Z⁰ Exchange

At $Q^2 \approx M_Z^2$ effects from Z^0 exchange cannot be neglected anymore



$$\frac{d^2\sigma_{NC}^\pm}{dx dQ^2} = \frac{2\pi\alpha^2}{Q^4 x} [Y_+ F_2(x, Q^2) \oplus Y_- x F_3(x, Q^2)] \quad (Y_\pm = 1 \pm (1 - y)^2)$$

$$F_2(x, Q^2) = F_2^\gamma - a_{\gamma Z} \kappa_Z F_2^{\gamma Z} + a_Z \kappa_Z^2 F_2^Z$$

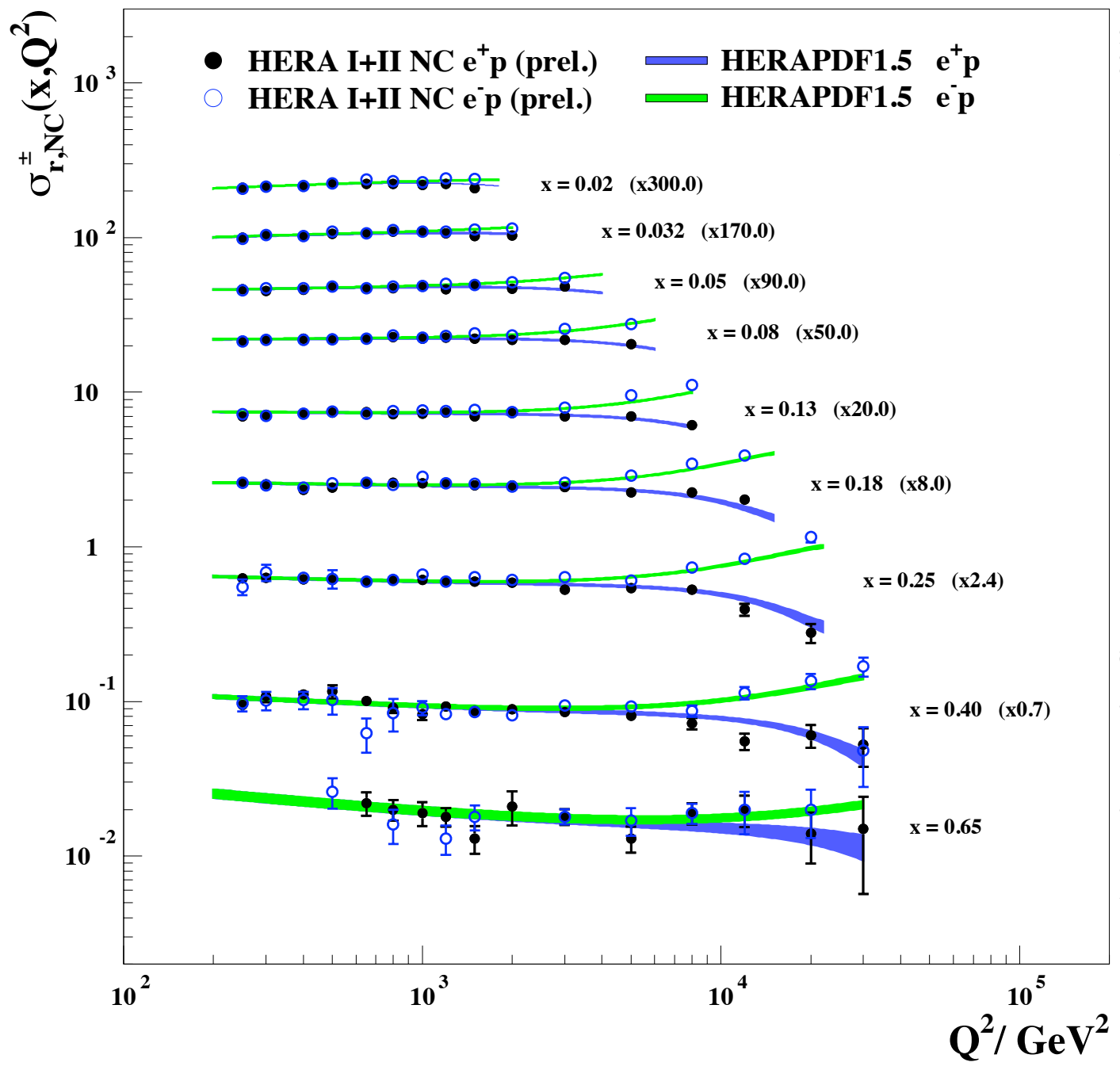
$$\kappa_Z = \frac{Q^2}{Q^2 + M_Z^2} \frac{1}{\sin^2 2\theta_W}$$

$$xF_3(x, Q^2) = -xb_{\gamma Z} \kappa_Z F_3^{\gamma Z} + xb_Z \kappa_Z^2 F_3^Z$$

Parity violating structure function

High Q^2 NC Cross Section and xF_3

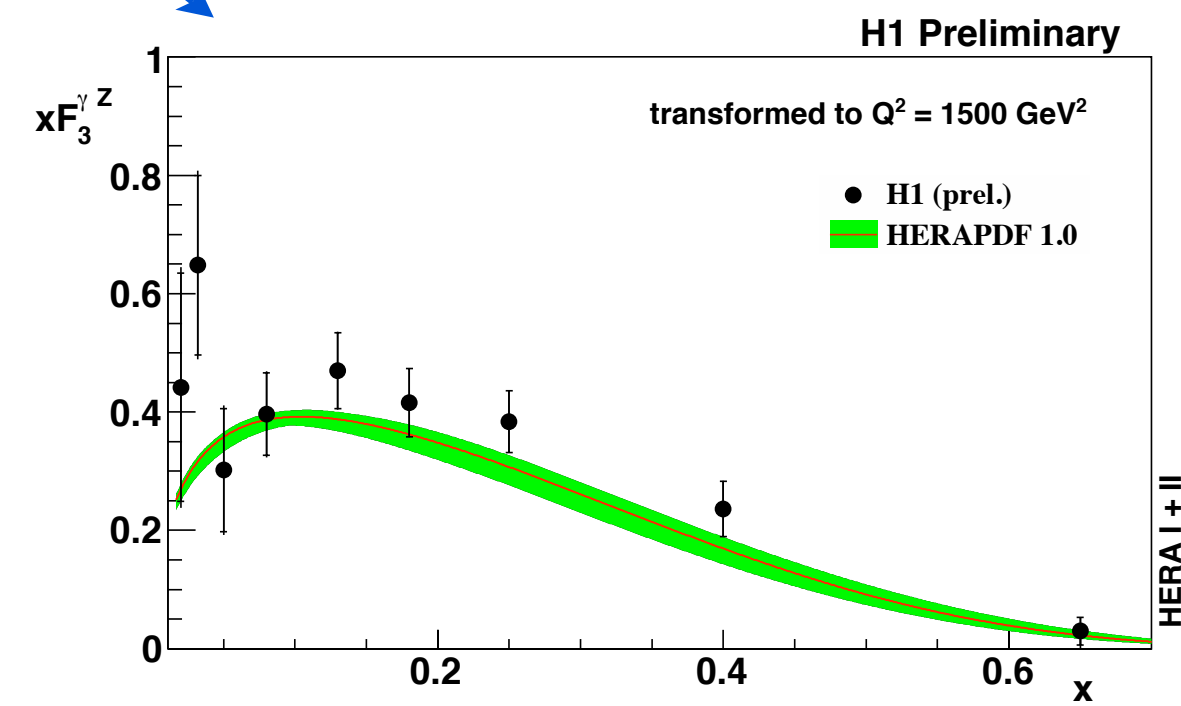
H1 and ZEUS



August 2010
HERA Inclusive Working Group

e^-p scattering:
positive interference
between γ and Z^0

e^+p scattering:
negative interference



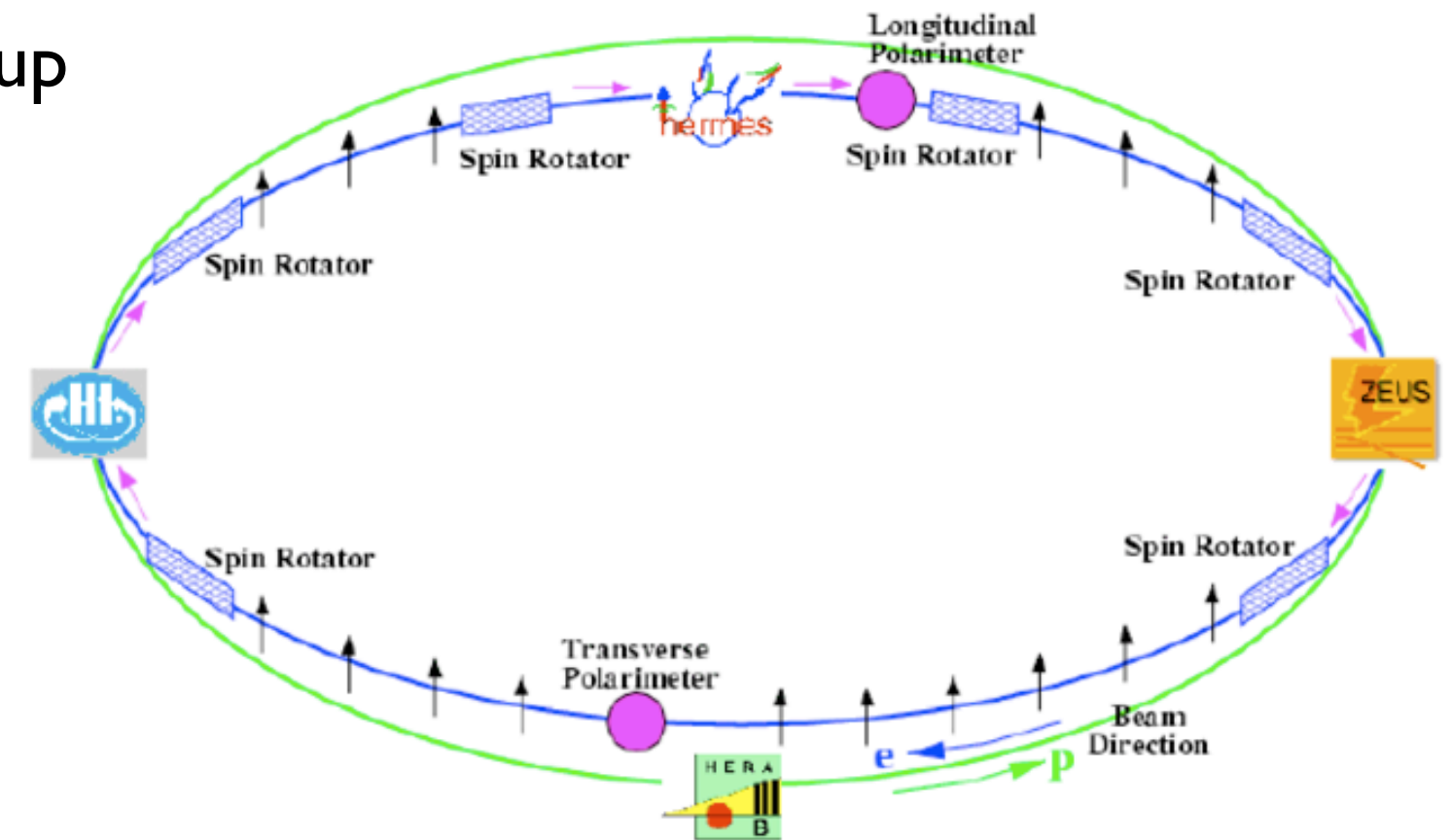
HERA I + II



Polarisation at HERA

Transverse polarisation builds up
due to synchrotron radiation
(Sokolov-Ternov effect)

At the upgrade HERA has
been equipped with spin
rotators

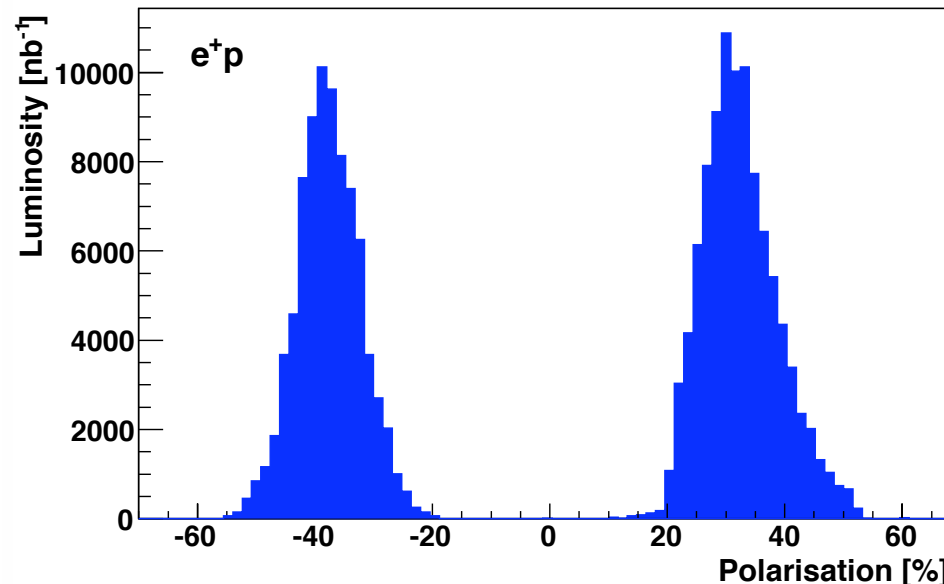


Spin rotator: flips transverse → longitudinal spin
before the experiments and back afterwards

Positive or negative helicity states can be achieved!

$$\text{Beam polarisation: } P_e = \frac{N_{\text{RH}} - N_{\text{LH}}}{N_{\text{RH}} + N_{\text{LH}}}$$

Polarisation at HERA



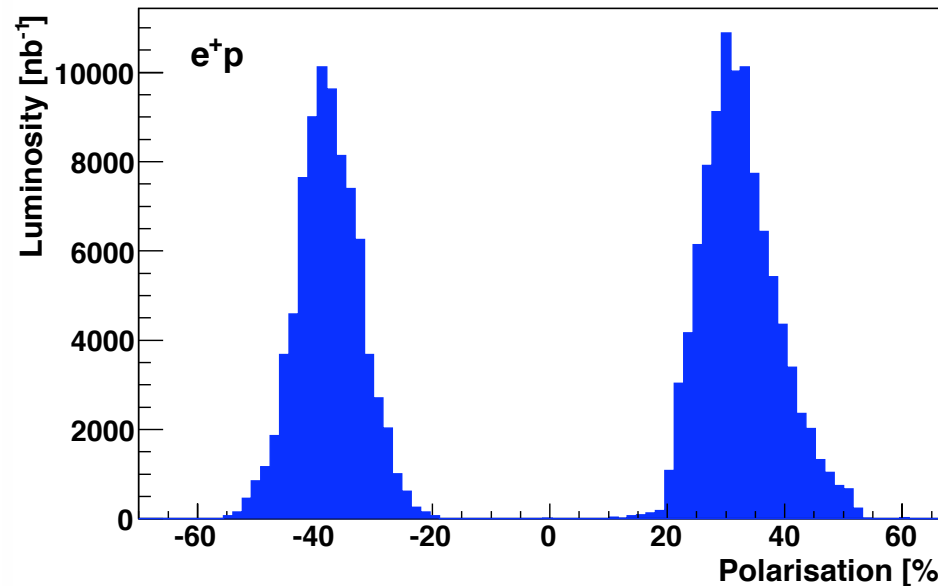
Example of polarisation: HERA-2
running with positrons

At HERA polarisation of ~30-55%
were achieved

The CC cross section depends on the longitudinal polarisation P_e :

$$\frac{d^2\sigma_{CC}^\pm(P_e)}{dx dQ^2} = (1 \pm P_e) \frac{d^2\sigma_{CC}^\pm}{dx dQ^2}$$

Polarisation at HERA



Example of polarisation: HERA-2 running with positrons

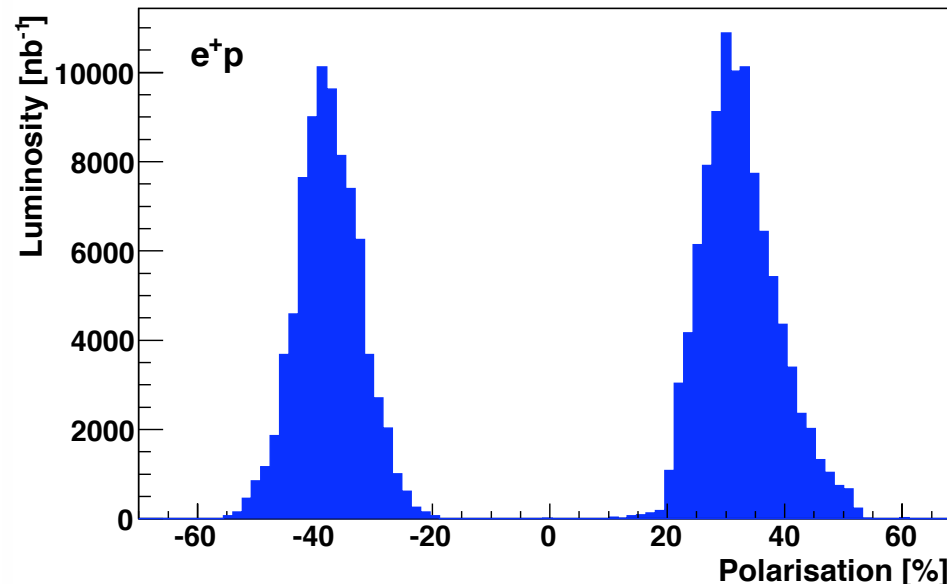
At HERA polarisation of ~30-55% were achieved

The CC cross section depends on the longitudinal polarisation P_e :

$$\frac{d^2\sigma_{CC}^\pm(P_e)}{dx dQ^2} = (1 \pm P_e) \frac{d^2\sigma_{CC}^\pm}{dx dQ^2}$$

Why?

Polarisation at HERA



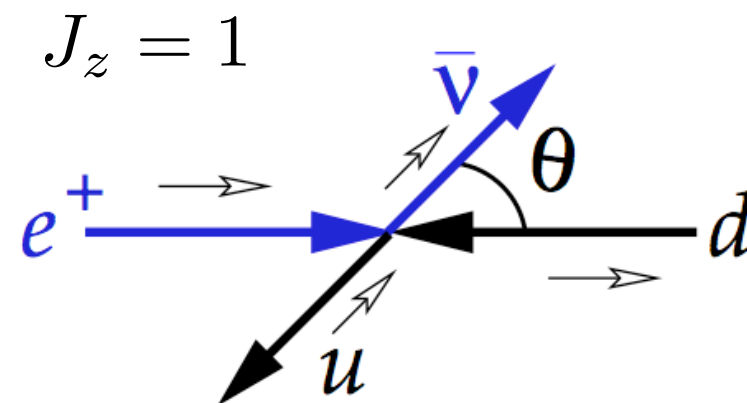
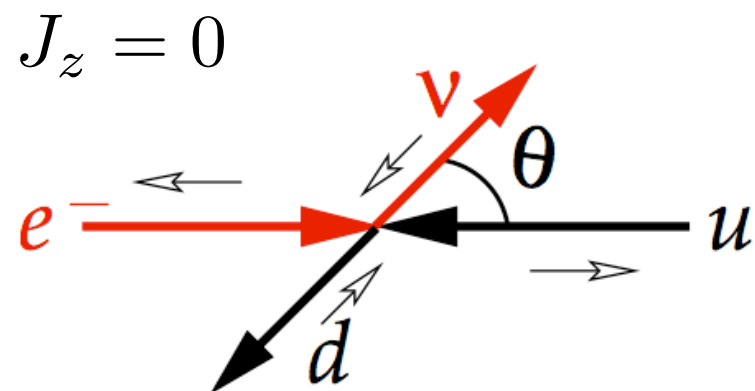
Example of polarisation: HERA-2 running with positrons

At HERA polarisation of ~30-55% were achieved

The CC cross section depends on the longitudinal polarisation P_e :

$$\frac{d^2\sigma_{CC}^\pm(P_e)}{dx dQ^2} = (1 \pm P_e) \frac{d^2\sigma_{CC}^\pm}{dx dQ^2}$$

Why?



No right-handed neutrinos (left-handed anti-neutrinos) in the SM!

Polarised CC Cross Section

Standard Model Expectation:

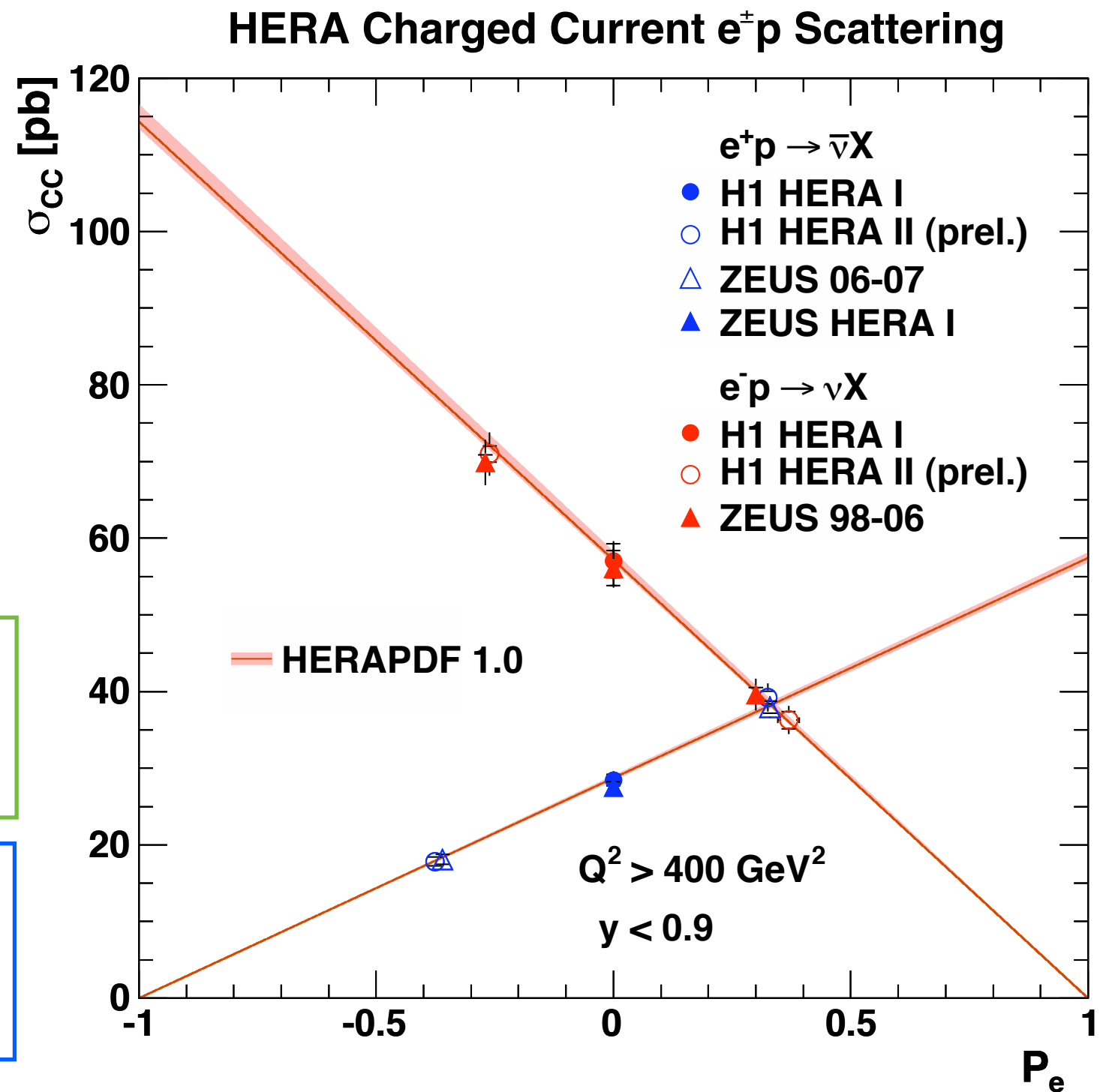
$$\sigma_{CC}^-(P_e = +1) = 0$$

$$\sigma_{CC}^+(P_e = -1) = 0$$

Observed (H1):

$$\begin{aligned} \sigma_{CC}^-(+1) &= -0.9 \pm 2.9_{\text{(stat)}} \\ &\quad \pm 1.9_{\text{(sys)}} \pm 1.9_{\text{(pol)}} \text{ pb} \end{aligned}$$

$$\begin{aligned} \sigma_{CC}^+(-1) &= -3.9 \pm 2.3_{\text{(stat)}} \\ &\quad \pm 0.7_{\text{(sys)}} \pm 0.8_{\text{(pol)}} \text{ pb} \end{aligned}$$



The Longitudinal Structure Function F_L

The longitudinal structure function F_L is defined as $F_L = F_2 - 2xF_1$

F_L describes the scattering of longitudinally polarised photons off a proton

In the QPM we found $2xF_1 = F_2 \Rightarrow F_L = 0$

F_L is non-zero in the QCD improved QPM, since partons can have non-negligible P_T

The NC cross section in its most general Form:

$$\frac{d^2\sigma_{\text{NC}}^\pm}{dx dQ^2} = \frac{2\pi\alpha^2}{Q^4 x} [Y_+ F_2(x, Q^2) \mp Y_- x F_3(x, Q^2) - y^2 F_L(x, Q^2)]$$

F_L is directly proportional to the gluon density: $F_L \propto \text{"}\alpha_s q + \alpha_s g\text{"}$

Measurement of F_L

Rewrite the NC cross section, neglecting xF_3 (contributes only at high Q^2)

$$\frac{d^2\sigma_{NC}}{dx dQ^2} = \frac{2\pi\alpha^2}{Q^4 x} (1 + (1 - y)^2) \left(F_2(x, Q^2) - \frac{y^2}{1 + (1 - y)^2} F_L(x, Q^2) \right)$$

or in terms of the reduced cross section:

$$\sigma_r(x, Q^2) = F_2(x, Q^2) - \frac{y^2}{1 + (1 - y)^2} F_L(x, Q^2)$$

Measurement of F_L

Rewrite the NC cross section, neglecting xF_3 (contributes only at high Q^2)

$$\frac{d^2\sigma_{NC}}{dx dQ^2} = \frac{2\pi\alpha^2}{Q^4 x} (1 + (1 - y)^2) \left(F_2(x, Q^2) - \frac{y^2}{1 + (1 - y)^2} F_L(x, Q^2) \right)$$

or in terms of the reduced cross section:

$$\sigma_r(x, Q^2) = F_2(x, Q^2) - \frac{y^2}{1 + (1 - y)^2} F_L(x, Q^2)$$

How could we measure it?

Measurement of F_L

Rewrite the NC cross section, neglecting xF_3 (contributes only at high Q^2)

$$\frac{d^2\sigma_{NC}}{dx dQ^2} = \frac{2\pi\alpha^2}{Q^4 x} (1 + (1 - y)^2) \left(F_2(x, Q^2) - \frac{y^2}{1 + (1 - y)^2} F_L(x, Q^2) \right)$$

or in terms of the reduced cross section:

$$\sigma_r(x, Q^2) = F_2(x, Q^2) - \frac{y^2}{1 + (1 - y)^2} F_L(x, Q^2)$$

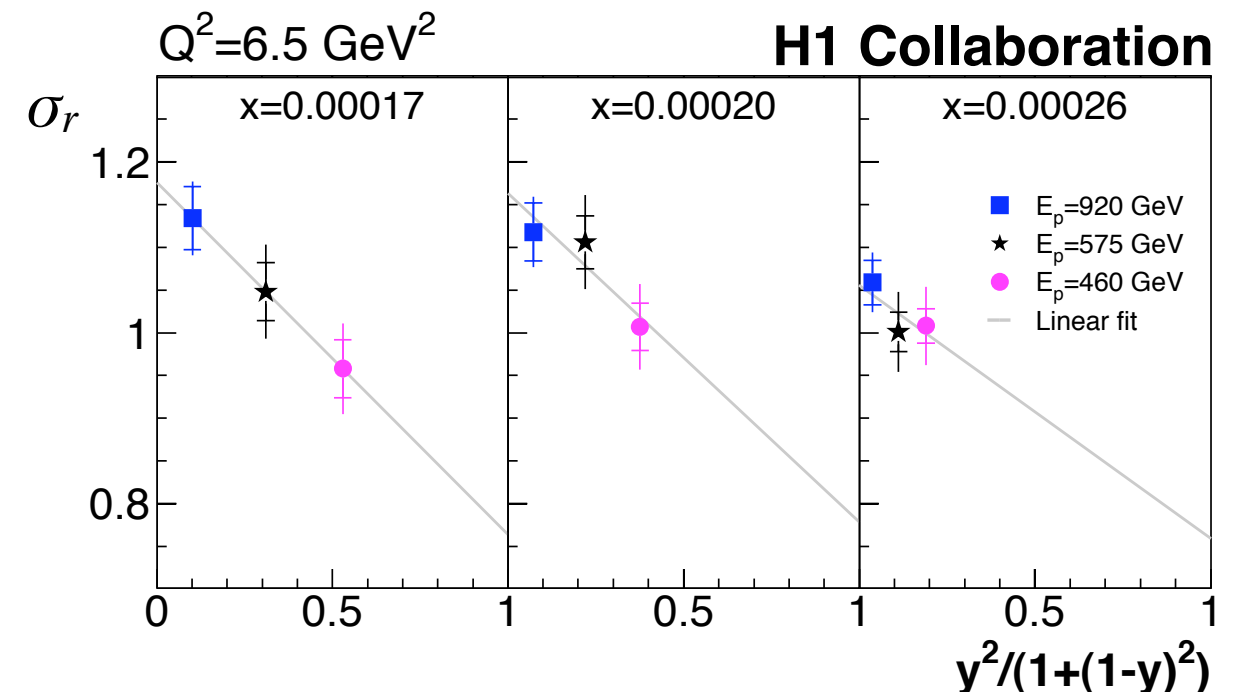
How could we measure it?

Measure σ_r at the same x and Q^2 , but at different values of y

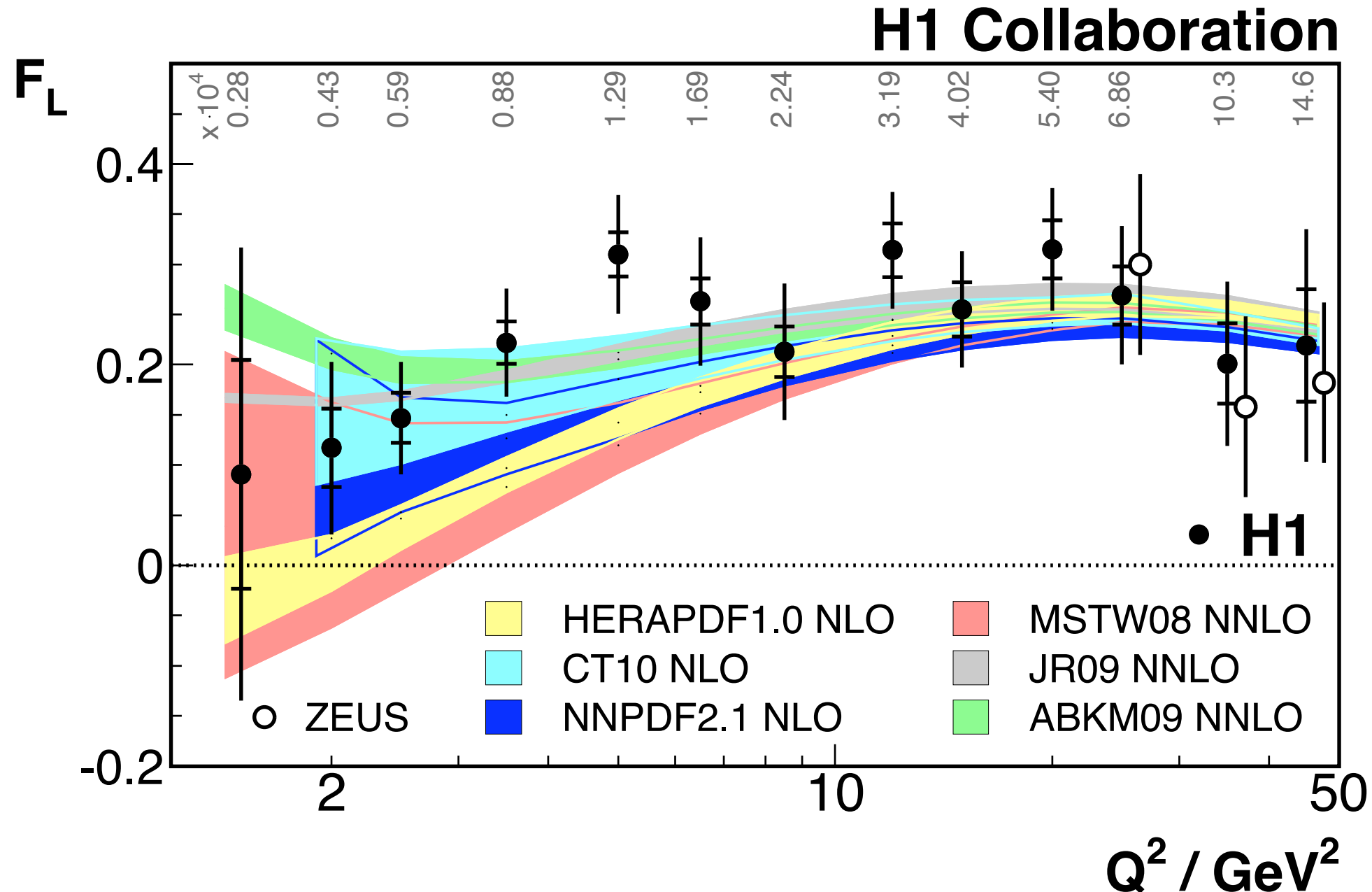
Determine F_L from the slope

Only possible with different s ,
since $Q^2 = xys$

⇒ Measure at different beam energies!



The Longitudinal Structure Function



F_L consistent with expectation from PDF fits and pQCD

More precise information on gluon from scaling violations

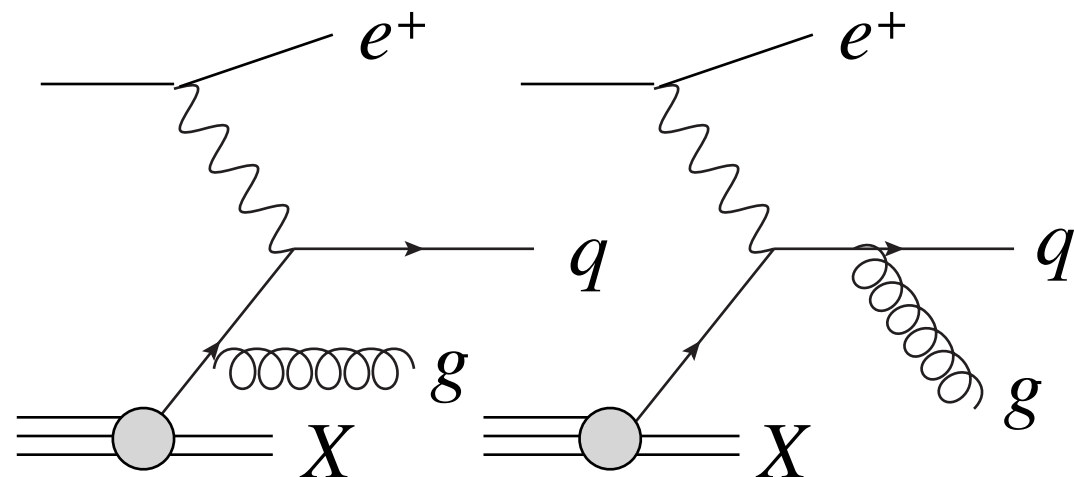
Exclusive Measurements

So far we have only looked at inclusive measurements - we measured the scattered electron and integrated over the final state X

Let's try to be a bit more exclusive and try to measure

$$e^+ p \rightarrow e^+ + q + g + X$$

We will have to consider contributions like

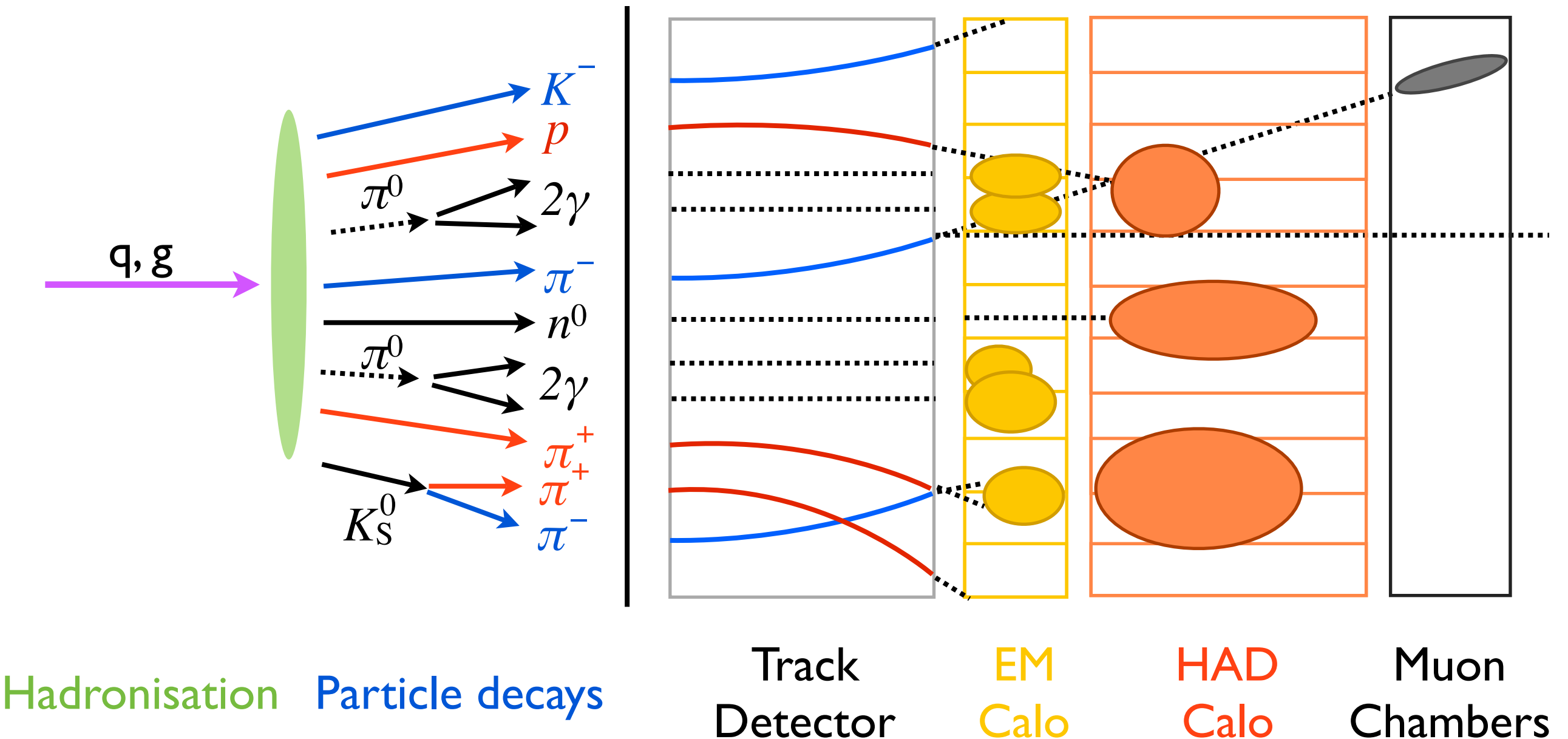


But:

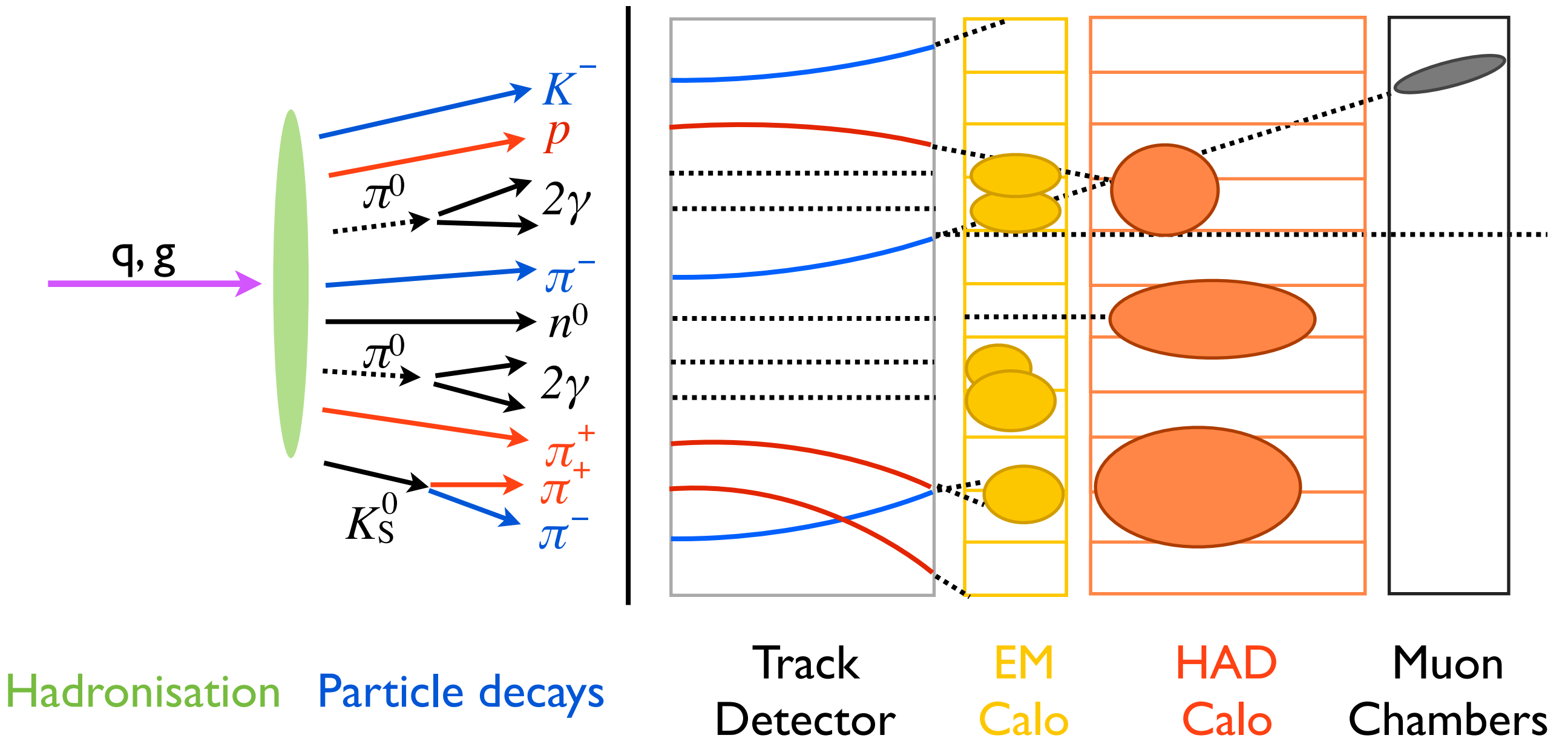
We can not measure these processes since quarks and gluons cannot be observed as free particles: we only see hadrons, leptons, photons...

We can not calculate these processes because of divergent integrals

What Can We Measure?



What Can We Measure?

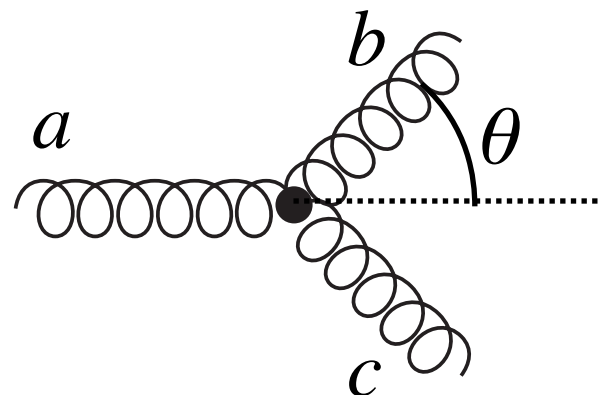


After the hadronisation and the detector effects it is virtually impossible to reconstruct all particles which originated from a single quark or gluon

The total deposited energy can be well measured

What Can We Calculate?

Timelike branching:



Gluon splitting on outgoing line b : $p_a^2 = E_b E_c (1 - \cos \theta)$

Propagator $1/p_a^2$ diverges when emitted gluon is soft (E_b or $E_c \rightarrow 0$) or when b and c are collinear ($\theta \rightarrow 0$) \Rightarrow Infrared (IR) divergences

Possible solutions:

- › Factorisable quantities
- › Infrared and collinear (IRC) safe observables
 - ◊ total cross sections
 - ◊ event shape variables
 - ◊ jets

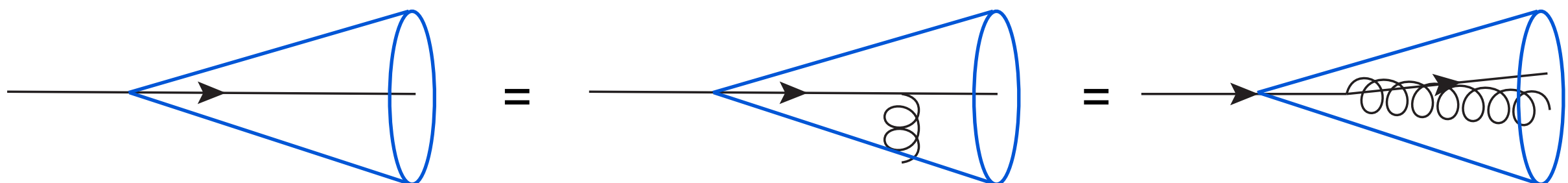
Jets

IRC safety: Observables insensitive to soft and/or collinear emissions

Divergences from virtual contributions (loops) cancel with divergent contributions from real emissions - KLN theorem

A jet algorithm combines objects (partons, hadrons, detector deposits) which are “close” together

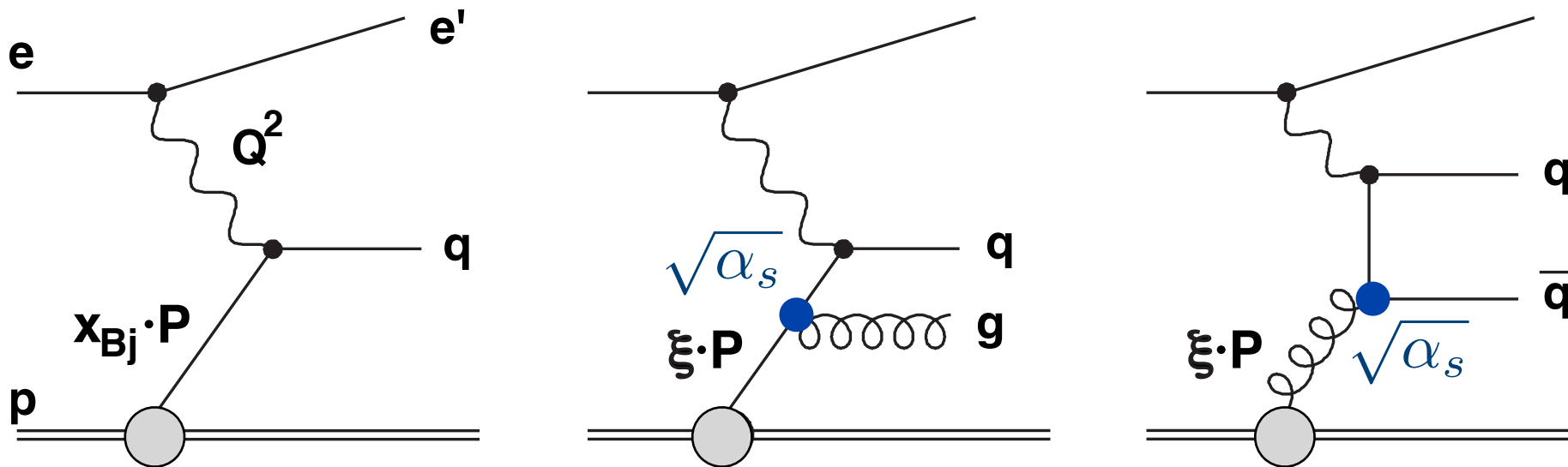
Different choices for IRC safe jet algorithms exist, with different distance definitions (lectures from T. Schörner and G. Steinbrück)



Jets can be defined on parton, hadron and detector level - one requirement is good correspondence between these levels

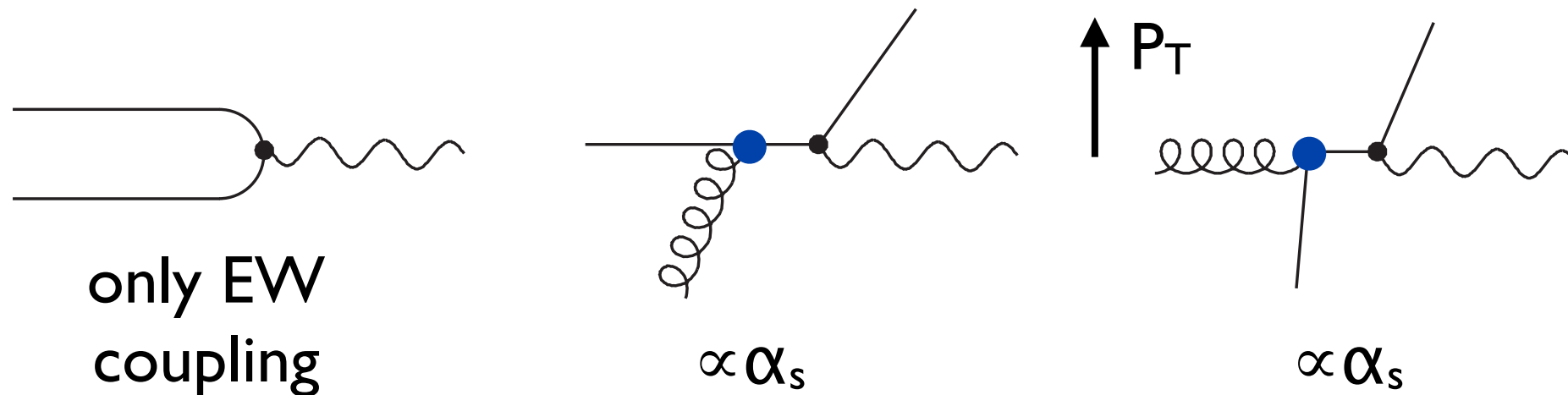
Jets help us to understand the underlying parton dynamics!

Jet Production In DIS



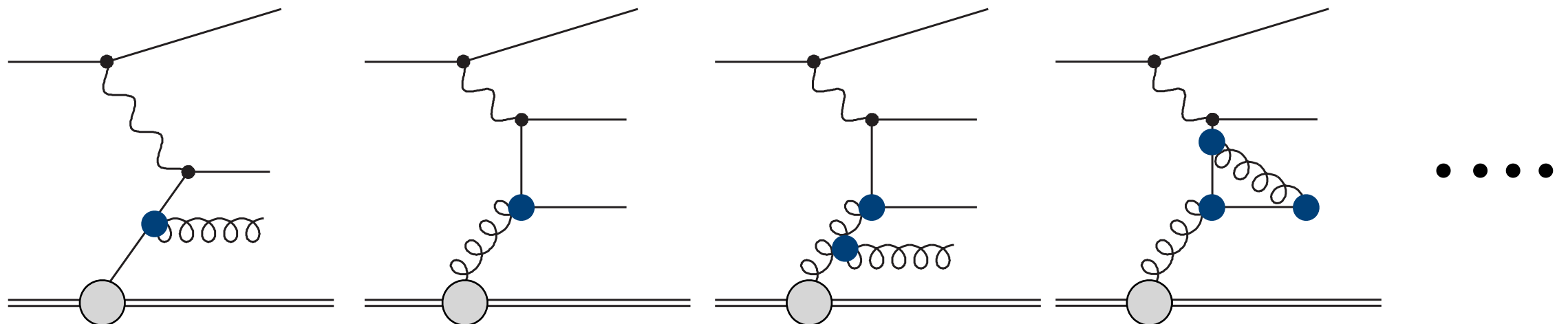
Momentum fraction of struck parton (in LO): $\xi = x \left(1 + \frac{M_{12}^2}{Q^2} \right)$

Boost to **Breit frame**, $2xP + q = 0$



Only hard QCD processes generate considerable P_T in the Breit frame
 n -jet production in LO $\propto \alpha_s^{n-1}$

Jet Production In DIS



$$\sigma_{\text{njet}} = \sum_{i=q,\bar{q},g} \int_0^1 dx \frac{f_i(x, \mu_f)}{\hat{\sigma}_i(x, \alpha_s^{n-1}(\mu_r), \mu_r, \mu_f)} (1 + \delta_{had})$$

$f_i(x, \mu_f)$: PDF of parton i in proton \Rightarrow test universality of PDFs

$\hat{\sigma}_i$: partonic cross section, calculable in pQCD up to NLO

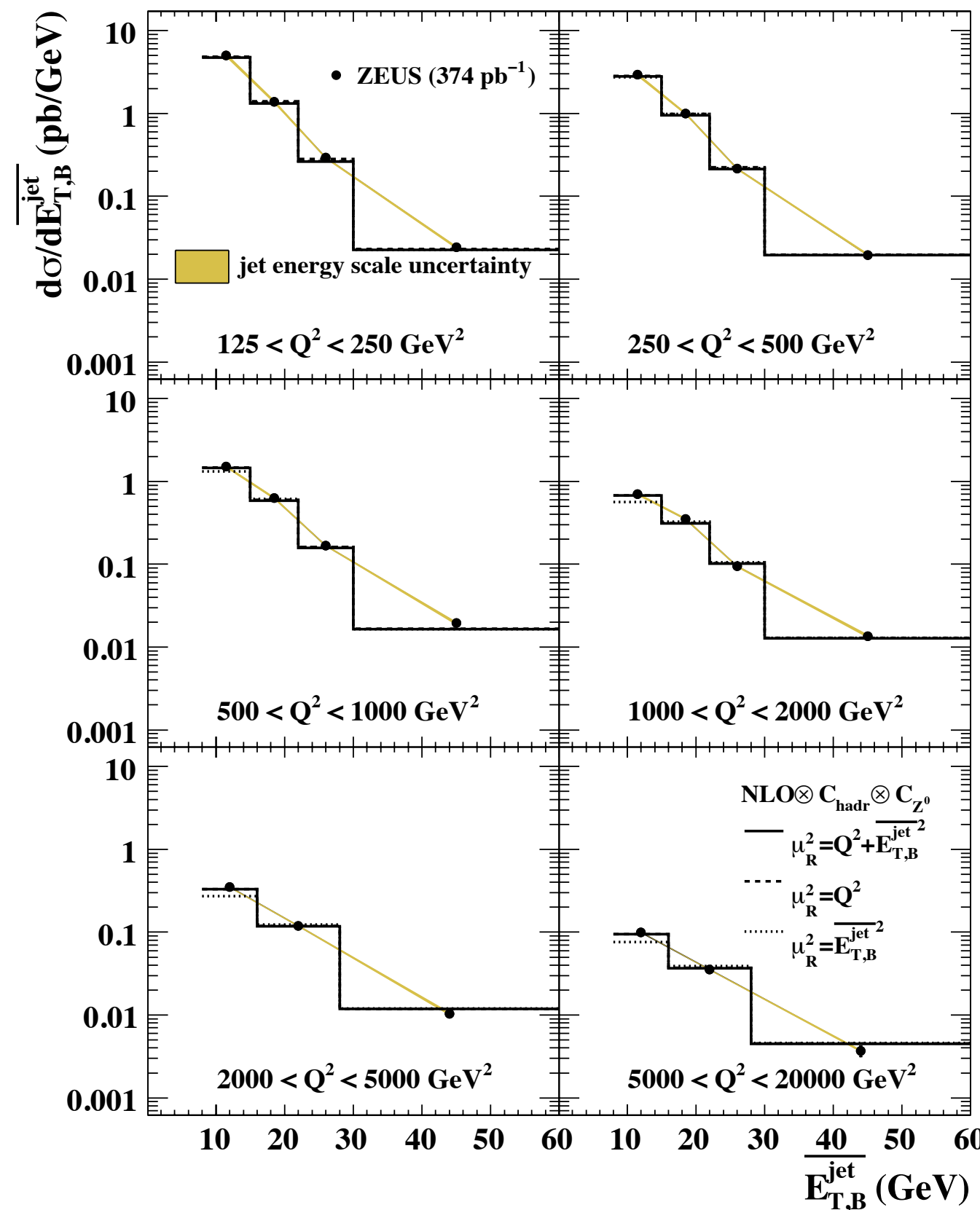
2-jet cross sections in LO: $\mathcal{O}(\alpha_s)$ and in NLO: $\mathcal{O}(\alpha_s^2)$

3-jet cross sections in NLO: $\mathcal{O}(\alpha_s^3)$

$(1 + \delta_{had})$: hadronisation corrections, obtained from different models

choice of scales: $\mu_f = Q$ $\mu_r = \sqrt{(Q^2 + P_T^2)/2}$ or $\mu_r = \langle P_T \rangle$

Dijet Cross Sections



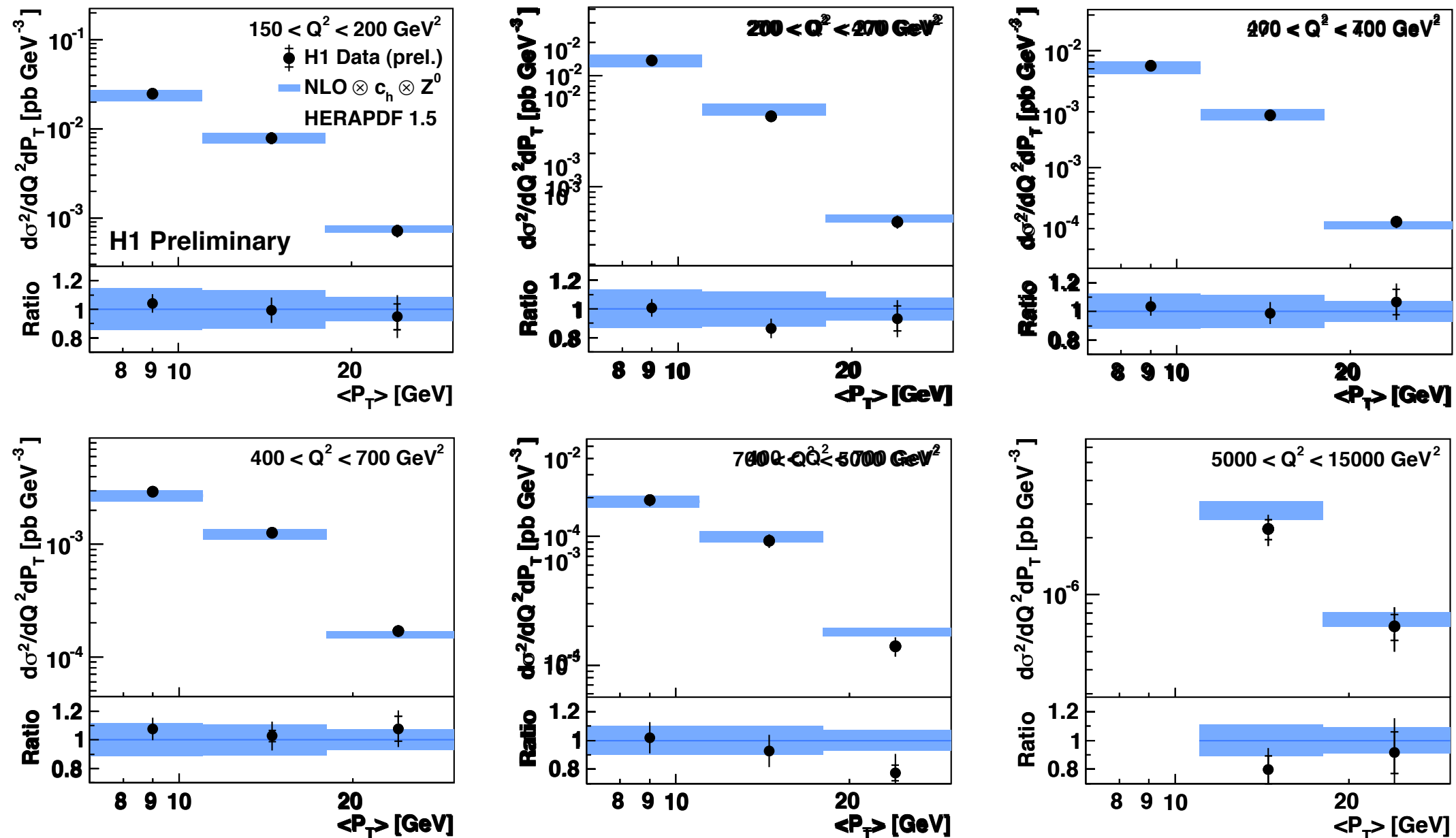
Measurement spans about three orders of magnitude

Stringent test of PDFs and perturbative QCD

Data are well described by NLO calculations over large range in Q^2 and P_T

Experimental uncertainty of 4-8% about half the theoretical uncertainty

Trijet Cross Sections

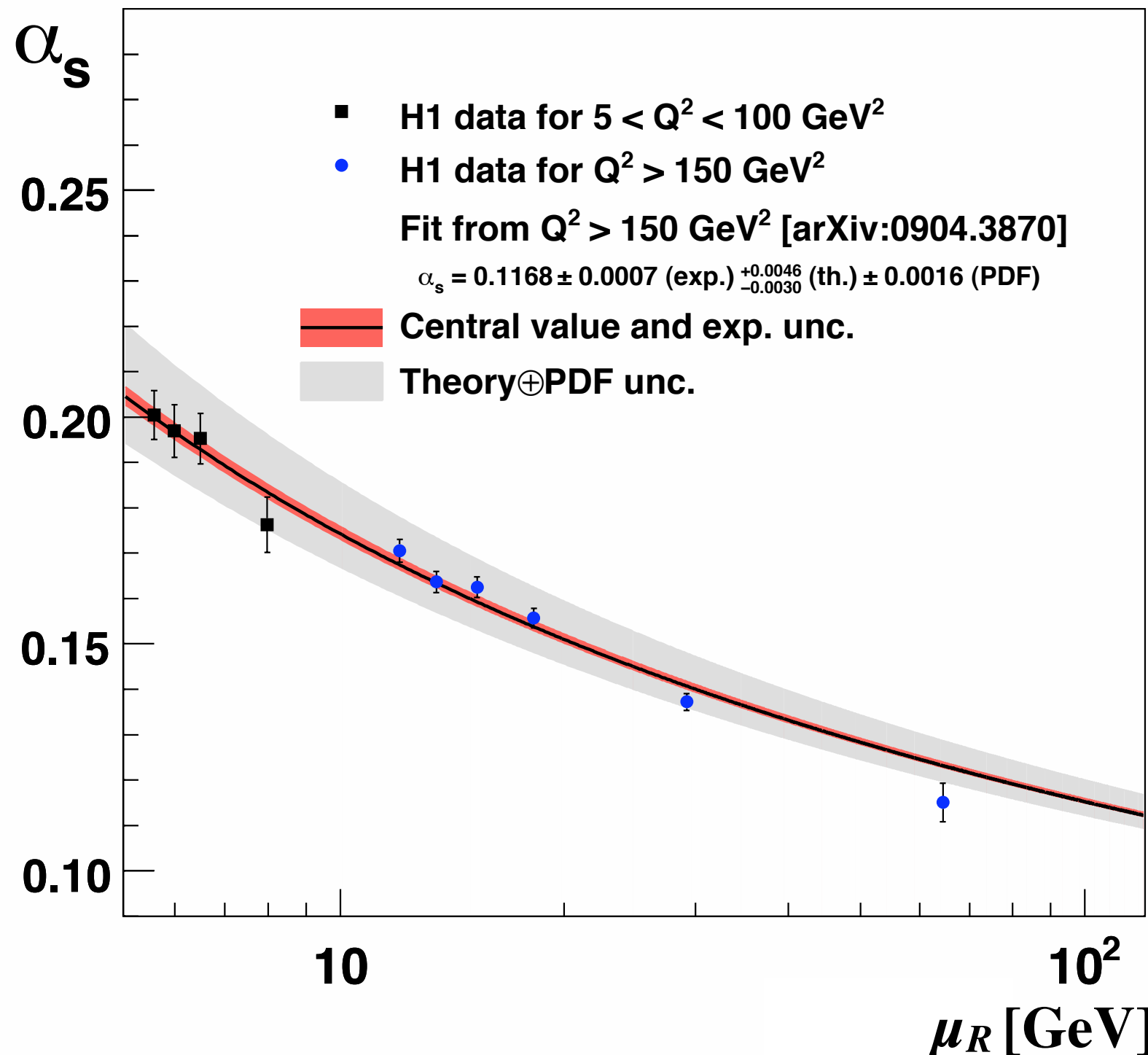


Double-differential trijet cross section measurement at high Q^2

Experimental uncertainty of 6% (low $\langle P_T \rangle$) and 15% (high $\langle P_T \rangle$)

α_s Determination From Jets

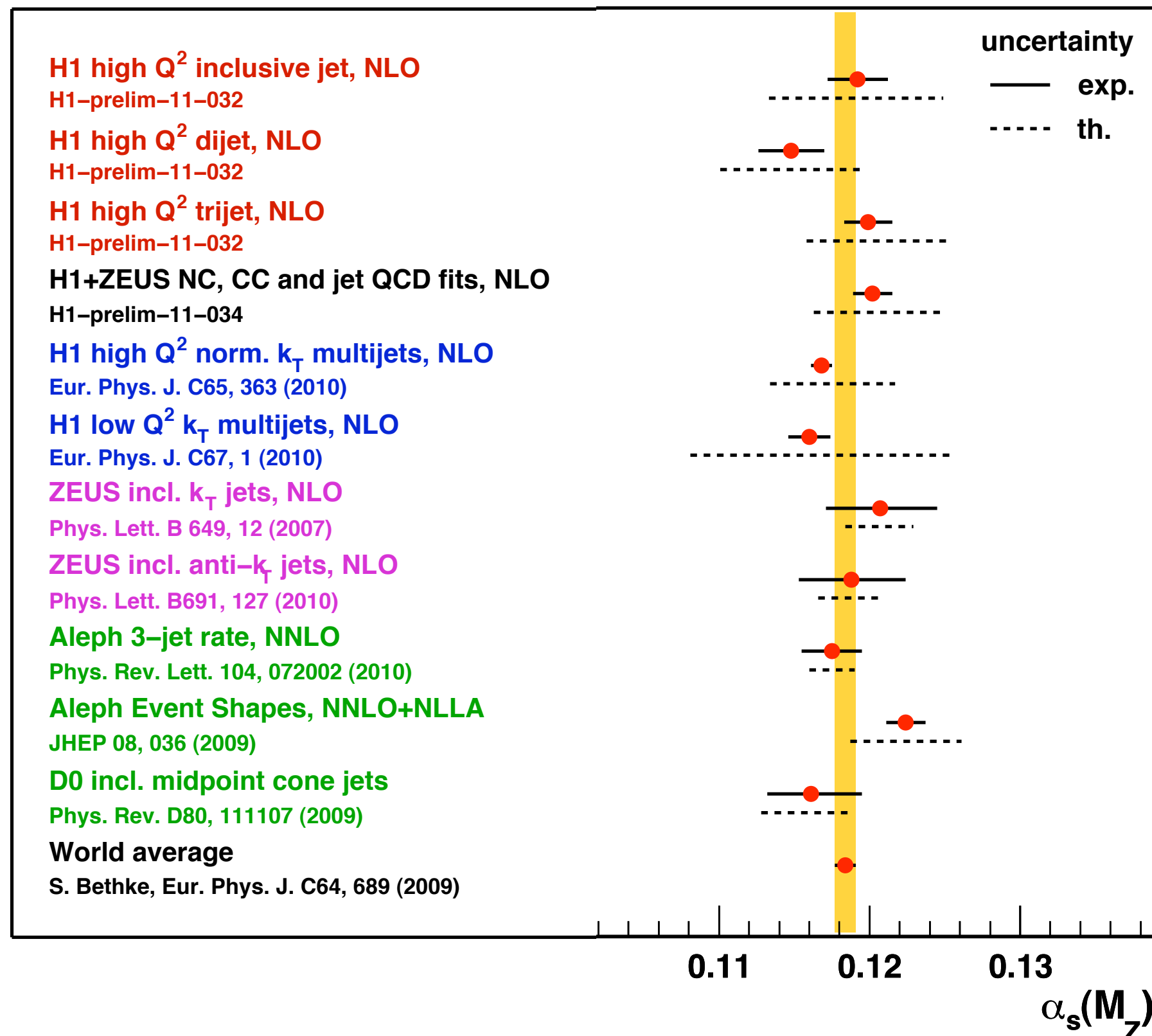
α_s from Jet Cross Sections in DIS



Running of $\alpha_s(\mu_R)$
measured over a large
range by a single
experiment

$$\begin{aligned}\alpha_s(M_Z) &= 0.1168 \\ &\pm 0.0007 \text{ (exp)} \\ &\pm 0.0038 \text{ (th.)} \\ &\pm 0.0016 \text{ (pdf)}\end{aligned}$$

α_s From Jet Measurements



Jets And PDF Determinations

In PDF fits the gluon is constrained through scaling violations

The gluon is always multiplied by α_s , $F_2 = "q + \alpha_s g"$

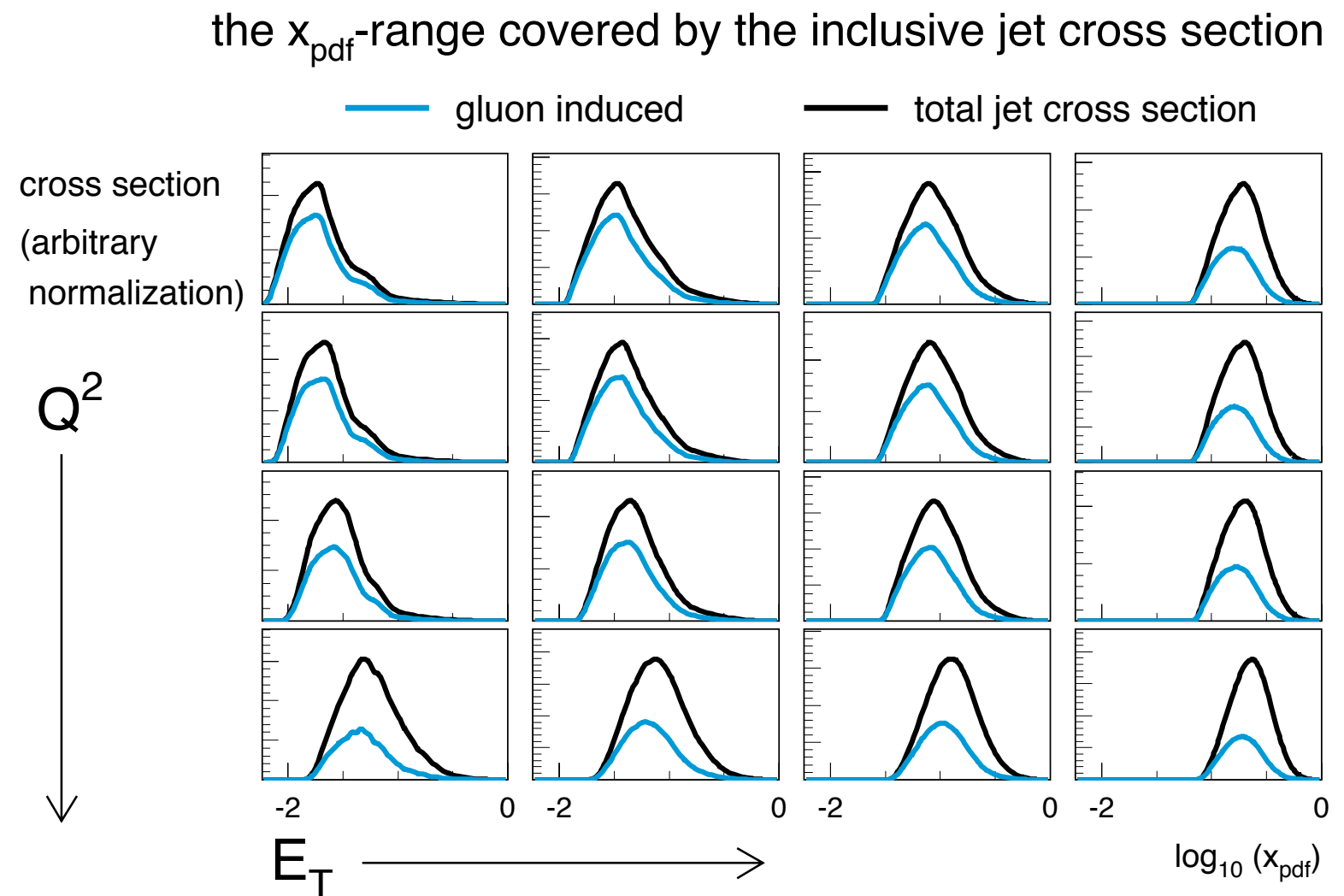
⇒ Strong correlation between gluon and value of α_s

Usually one keeps the value of α_s fixed in PDF determinations, then the gluon can be well constrained.

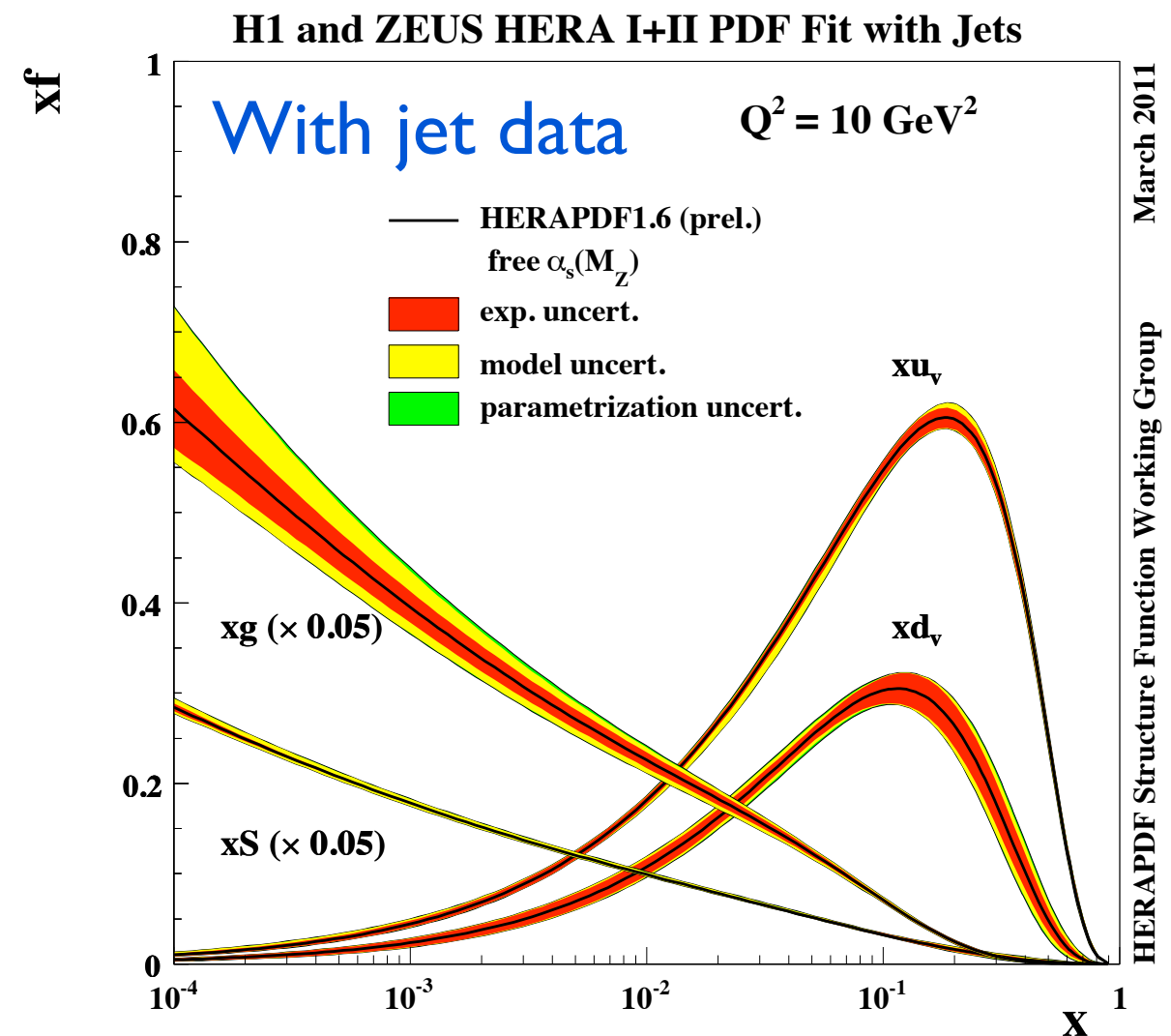
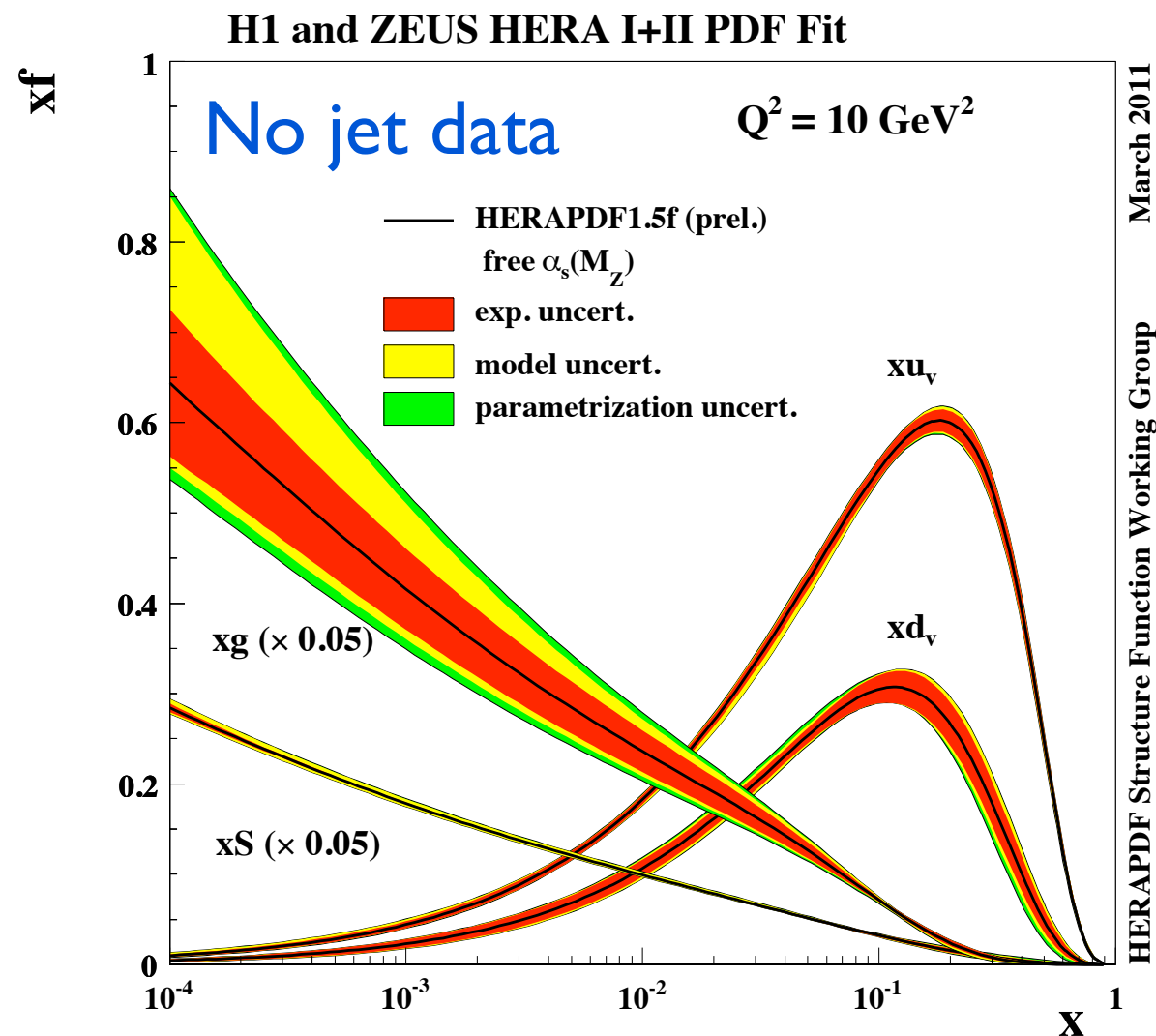
Jets can decorrelate the gluon and α_s :

low Q^2 : $\sigma_{\text{jet}} \propto " \alpha_s g "$

high Q^2 : $\sigma_{\text{jet}} \propto " \alpha_s q "$



PDFs With $\alpha_s(M_Z)$ As Free Parameter

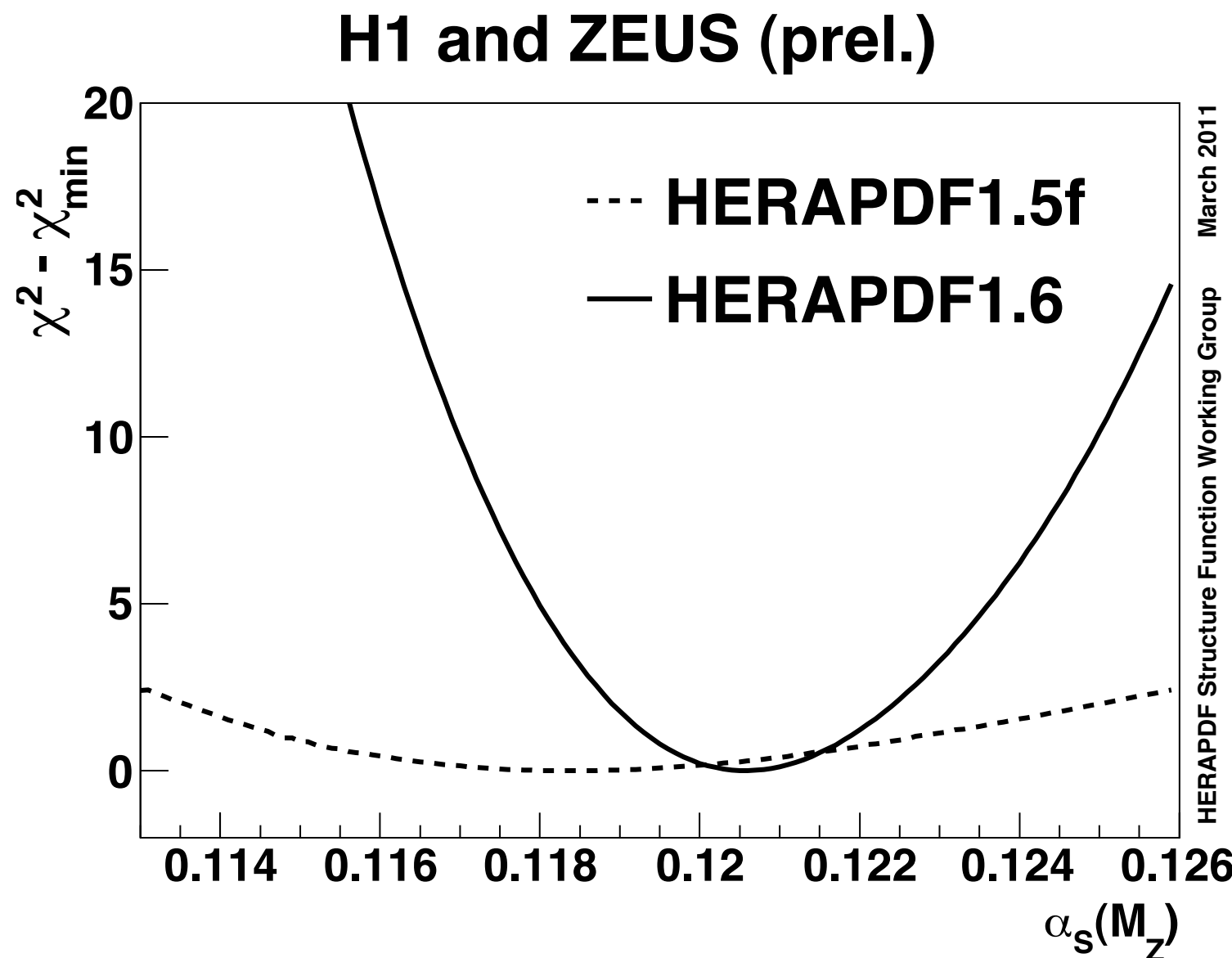


Uncertainty of gluon PDF becomes large when $\alpha_s(M_Z)$ is left free in fit

Jet data helps to decorrelate the gluon from α_s during the fit

PDF Fit: χ^2 Versus α_s

Turn the argument around: how well can we determine $\alpha_s(M_Z)$ when the gluon is left free?



- dashed line:**
PDF determination with α_s as free parameter, no jet data
- solid line:**
same as above, but including jet data in the fit

$$\chi^2_{\text{min}} / \text{n.d.f} \approx 1.04$$

α_s is well constrained in a simultaneous fit

HERA Physics

(we have not covered much)

The structure of the proton

- › Structure functions, parton density functions (PDFs), spin...

Electroweak Physics

- › Charged current interactions, EW unification...

QCD

- › Jets, α_s , heavy quark production, hadron production...

The structure of the photon

- › $\gamma^* p$ scattering, photoproduction...

Searches for physics beyond the standard model

- › SUSY, leptoquarks, contact interactions...

Diffraction

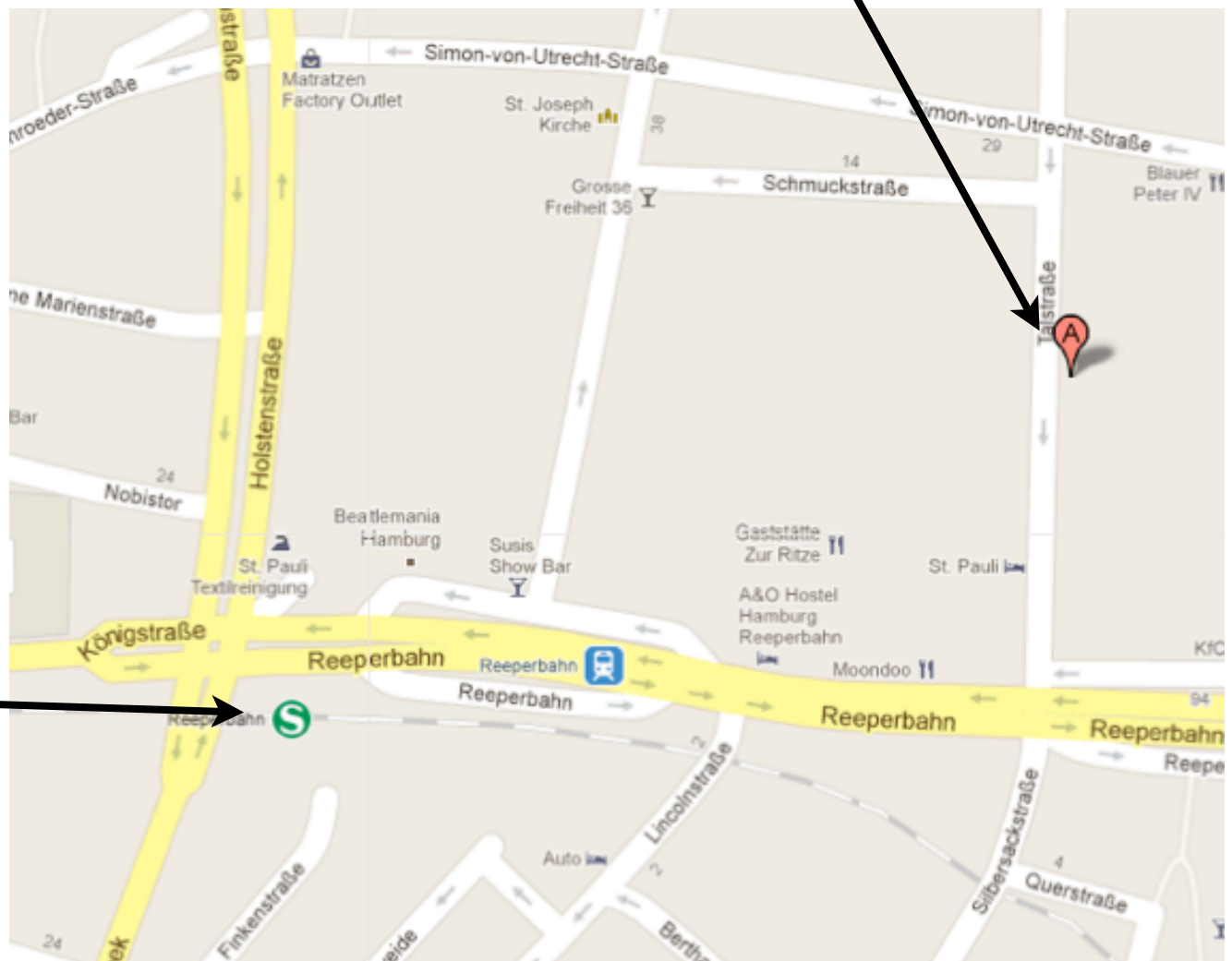
- › Diffractive structure functions, diffractive particle production...

Chat About Physics, Hamburg, Music and Anything Else: Tonight



Roman
at ~21.00h

3 Zimmer Wohnung
Talstrasse 22



S-Bahn Station
Reeperbahn